Performance analysis of Graphite and Multi Wall Carbon Nanotube based Counter Electrodes in Dye Sensitized Solar Cells

M.S. THESIS

September, 2016

A thesis on

Performance analysis of Graphite and Multi Wall Carbon Nano Tube based Counter Electrodes in Dye Sensitized Solar Cells

A thesis is submitted to the Institute of Energy, University of Dhaka in partial fulfillment of the requirements for the Degree of Masters of Science in Renewable Energy Technology

By

Kanij Raihana

4th Batch

Roll: 522

Session: 2014-15

September, 2016

Declaration

It is hereby declared that this thesis or any part of it has not been submitted elsewhere for the award of any degree or diploma.

As far of my knowledge

Signature of the Student

Kanij Raihana

Signature of the Supervisor:

Dr. S.M. Nasif Shams

Associate Professor
Institute of Energy
University of Dhaka

Signature of the co-Supervisor:

Dr. Mubarak Ahmad Khan

Director General
Atomic Energy Research Establishment
(AERE), Saver

Signature of the Co- Supervisor:

Dr. Md. Mosharraf Hossain Bhuiyan

Principal Scientific Officer (PSO)
Institute of Nuclear Science & Technology
Atomic Energy Research Establishment (AERE), Savar

Acknowledgement

First and foremost, I would like to thank ALLAH, the Almighty without whom I would not have been here and I am thankful for his unconditional love & mercy.

Secondly I would like to thank Dr.S.M. Nasif Shams, Associate Professor, Institute of Energy, University of Dhaka; my supervisor, he found time to support and advice amidst his already filled up daily schedule and also to my co-supervisors, Dr. Mubarak Ahmad Khan, Chief Scientific officer (CSO), Atomic Energy Research Establishment (AERE) ,Dr. Md. Mosharraf Hossain Bhuiyan, Principal Scientific Officer (PSO), INST, Atomic Energy Research Establishment (AERE) for their kind co-operation and supervision. I am also thankful to Jahid M.M. Islam. Besides, I want to convey my gratitude to Md. Saifur Rahman, Scientific Officer, IRPT, AERE for his guidance and support during the period of the research work. My sincere thankfulness to the research assistants of the DSSC project Tania Akhter, Tauhidul Islam, Toriqul Islam Bhuiyan for their immense help in the experimental work.

I further extend my heartfelt gratitude to my parents whose words of advice, care and support have brought me here and whose loves have kept me going.

Lastly thanks to IDCOL for providing financial support under AERE-IDCOL solar cell project for completion of this research work. In addition, thanks to Ministry of Science & Technology, GOB, for providing partial support under special allocation for this research work.

Table of Contents

Table of Figures

ABSTRACT

In this research work, a new type of cost-effective metal-free counter electrode for dye sensitized solar cell is introduced. This new type of solar cell is environment friendly in nature which has been investigated by the researchers. Recently DSSC is becoming very popular due its organic nature and its flexible application in various fields. It can be integrated in building integrated photovoltaic cell, act as a window glass, can be a portable charger for electronic gadgets. The overall structure of the cell is a sandwich-like formation that has photo sensitized anode in the first part and counter electrode at the end. Here 4 types of counter electrode is prepared by doctor blade technique where graphite and multi-wall carbon nanotube mixture follows 4 different ratios of 0:3, 3:0, 3:1 and 3:1 (with PEG) on a 2×1.6 cm^2 indium-doped tin oxide substrate. The counter electrode is expected to show enhanced electro catalytic characteristics toward reduction reaction as well as low charge-transfer resistance at the counter electrode-electrolyte interface. In combinationwith a natural dye (Indian Blackberry), dye-sensitized TiO_2 photo anode and a liquid electrolyte, the fabricated counter electrode DSSCs show 0.041%, 0.006%, 0.0139% and 0.0832% energy conversion efficiencies under 1 sun illumination ($100mW/cm^2$, 1.5AM). The data is comparable to the efficiency of the DSSC with platinum electrode that is 0.01% under the same experimental conditions. Hence the finding suggests that graphite and MWCNT (with PEG) ratio of 3:1 is a promising alternative counter electrode for low cost dye sensitized solar cells.

Chapter-1: Introduction

Now-a-days the most serious problems worldwide is the energy crisis as a result of increasing demands of modern lifestyle and technology. To fulfill this rising global demands natural resources such as oil, coal, natural gases are used as the resources for world energy supply. However these resources are limited and it is also causing severe damages to our environment [1].Also natural resources will take thousands of years to form and it cannot be replaced as fast as they are being consumed. As a result for finding alternative source of energy renewable energy step forward. Over the past few decades, various renewable energy sources from nature have been developed and used to supply the energy demands. Among them producing electricity from the sun may be the most ideal source because of its enormous electricity production [2].

Photovoltaic (PV) cells are photonic devices that traps sunlight, converts photon with specific wavelengths to electricity. Solar cells are categorized under the following three generations: 1) silicon-based (Si) solar cells, 2) thin film solar cells, 3) organic solar cells. The first generation Si-based solar cells are commercially available due to high efficiency. Nevertheless the complex manufacturing processes and high production costs urges to find cost efficient and eco-friendly solar cells to substitute the conventional PV cells. In 1991 Michael Gratzel developed a new type of organic photovoltaic cell by using organic dyes to sensitized comparatively inexpensive semiconductors which gave a significant energy conversion improvement to 7.9% [3]. Since their initial discovery, dye-sensitized solar cells (DSSCs) have attracted considerable attention as cost-effective photovoltaic systems. It can provide transparent and flexible solar cells and operate at high efficiencies at low light intensities, including scattered, angled, or shaded light.

This chapter intends to give information about the thesis work. Section 1.1 provides the main objectives of the thesis work. Section 1.2 informs about the motivation of thesis. Section 1.3 gives thesis outline.

1.1 Objective

This thesis work is experimental by nature and its main objective was to identify cost effective materials to use as counter electrode instead of platinum. However the specific activities in this thesis includes as follow:

1. Development of cost-effective methods and materials to prepare counter electrode.

2. Understanding the relationship between new materials and device performance by characterizing them in scanning electron microscopy, UV-visible spectroscopy.

3. Identify parameters that affect device performances and their optimization.

4. Comparison of 4 types of counter electrodes with platinum counter electrode based on overall performance with blackberry dye.

1.2 Motivation of Study

With the increase of world population, demand in energy sector is escalating day by day. Thus energy generation through fossil fuel is run out eventually. Thus solar energy is assumed to be an endless source for power generation. Solar cells are the medium to convert the sunlight into electricity. The majority of the solar cells are made from crystalline silicon. However some other materials are mercury, lead and cadmium telluride. Some of the materials are toxic which expose threats to the environment as well as public health.

Some of the materials used for manufacturing solar panel are rare elements such as telluride, ruthenium[4]. These materials are highly expensive because of their scarcity causing another drawback for conventional solar cell.

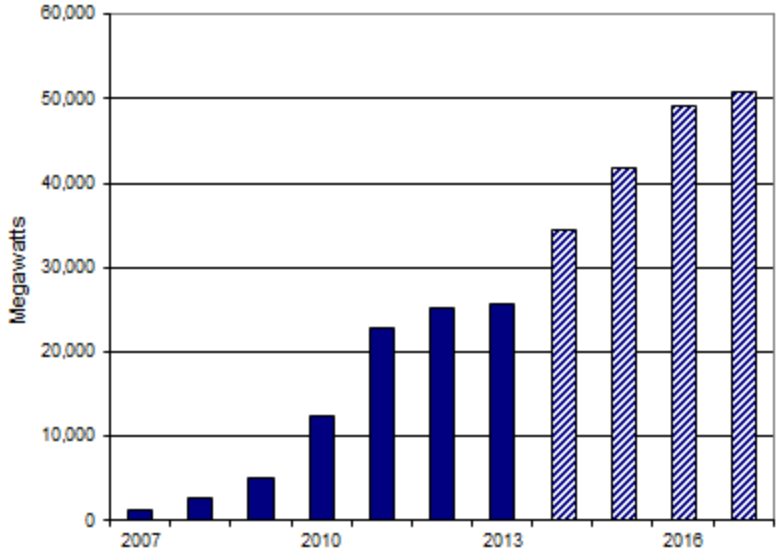

Figure 1: Annual PV module production in China 2007-2013, with projection of 2017

Moreover some of the materials are toxic as that possess potential risk for environment if not handled carefully. Industry workers may be the victim of these toxic materials if not handled carefully. Also incorrect way of disposal and recycling of photovoltaic modules are unsafe for environmental sustainability. There are processes for recycling the PV modules nonetheless no accurate information are available of their proper use in industries. All of a sudden the production of PV module rises as a consequence of their popularity as natural source energy. Thus large amount of modules are manufactured currently which is shown in Fig-1. But there is no such data of assuring their proper recycle. Therefore it still holds threat to environment pollution despite of its several advantages. Hence the thesis focuses on introducing new type of solar cell for their organic, eco-friendly nature with motivation to reduce environment pollution.

1.3 THESIS OUTLINE

Rest of the thesis parts is organized as follows:

Chapter 2: This chapter describes the history and progress of dye sensitized solar cells. Moreover it presents the advantages, disadvantages and applications of DSSC. It also includes general descriptions of the required materials needed for fabrication.

Chapter 3: This chapter focuses on the experimental method and procedures that are followed to fabricate counter electrodes. Also later of this chapter full cell assembly is also mentioned.

Chapter 4: This chapter provides characterization information of the fabricated counter electrodes.

Chapter 5: This chapter presents the electrical properties of the fully fabricated cells by investigating voltage and current data. Besides explanation of I-V curve is also given.

Chapter 6: This chapter provides the summery of the findings of this research work. Furthermore some suggestions and ideas are given for future research.

Chapter -2: Literature Review

This chapter aims to review the Dye sensitized solar cells as well as the history and development phase of solar cells. In section 2.1 focuses are given on the current researches of counter electrodes for DSSC. In section 2.2 the operating principle of the DSSC is outlined with a short review of DSSC. Section 2.3, 2.4, 2.5 discusses the advantages, disadvantages and its application in worldwide accordingly. Section 2.6 gives a short overview of the fundamental chemicals and materials that are generally used to fabricate DSSC. Lastly an overall review of this chapter is provided in section 2.7.

2.1 Literature review

Dye-sensitized solar cells (DSCs) have attracted extensive attention as a low-cost alternative to Si solar cells. A typical DSC consists of a photo anode and a counter electrode separated by an electrolyte containing an iodide/triiodide (I^-/I^{3-}) redox couple. Counter electrode is one of the most important parts because it collects the photo generation electrons from an external circuit and simultaneously regenerates dye sensitizers by reducing the Iodide electrolyte used.

In a typical counter electrode, Platinum (Pt) is used as a catalyst because of its high electrochemical activity [5]. However due to its high cost and paucity, Pt has to be replaced with other abundant and cost-effective materials that possess good catalytic properties for the reduction of the redox electrolyte and high conductivity for quick electron transport. Previous studies have revealed that carbonaceous materials including graphite, carbon black, carbon nanotubes can exhibit comparable electro catalytic performance to Pt for the reduction of I^{3-} ions [6]. It is noteworthy that carbonaceous materials are abundant and low-cost and also possess high resistivity against corrosion [7]. Recently, Murakami et al. reported carbon black-based counter electrodes in DSSCs and a remarkable conversion efficiency of approximately 9% under 100 mW/cm^2 was achieved [8].

Different forms of carbon materials have been studied as a less-expensive and stable catalyst for I^{3-} reduction reaction in DSSCs. In research a lot of attention has been paid to the synthesis, characterization and application of carbon nanotube (CNT) due to the unique structural, mechanical and electronic properties of the materials [9]. CNTs were studied either as supports or catalysts. As a support, CNTs showed more advantages in some catalytic reactions than the conventional supports besides, the mechanism of CNTs as catalytic materials is gaining more attention [10].

One of the inspiring works carried out by Lee et al. by MWCNT as an electro catalyst in the counter electrode of a DSSC [11]. Their DSSCs fabricated with MWCNT counter electrodes attained 7.67% efficiency whereas the conventional Pt-based cell obtained 7.83 % efficiency. Usually MWCNTs are coated on FTO glass that is used as a CE for DSSCs. In order to fabricate

MWCNT-coated FTO glass CEs, various techniques such as doctor blade, screen printing, spin coating, spray coating processes, and hydrothermal deposition have been developed.

Another alternative option is graphite-based counter electrode that often exhibit a low catalytic activity toward the redox couple. However graphite electrode can exhibit improved performance by adjusting their particle size and film thickness [12]. Graphite particles of large size and low surface area show very poor catalytic activity as CE materials [13]. This is because large graphite particles have fewer edge planes which slows the rate of I^{3-} reduction due to the high charge transfer resistance (R_{CT}). The high R_{CT} has a negative influence on the fill factor (FF) and shows poor energy conversion efficiency [12].

To provide similar performance to Pt counter electrodes a large surface are is required. Hence it is difficult to obtain high efficiency with carbon based counter electrodes. In this thesis report, demonstration is done for pt-free counter electrode that can be prepared from MWCNT and graphite. Further we systemically investigate the effect of fabricated MWCNT and graphite thin films on the photovoltaic performance of the resulting DSSCs.

2.2 Overview and Operating Principle of Dye Sensitized Solar Cell

The components of a DSC are: two conductive glass electrodes, usually coated with fluorine doped tin oxide (FTO-glass). One of the electrodes is the anode, which is screen printed with TiO_2 nanoparticles (particle size around 20-50 nm). The TiO_2 is sensitized with a dye, which absorbs the photons. The other electrode is the counter electrode (CE) and in between the two electrodes is the electrolyte containing the redox couple.

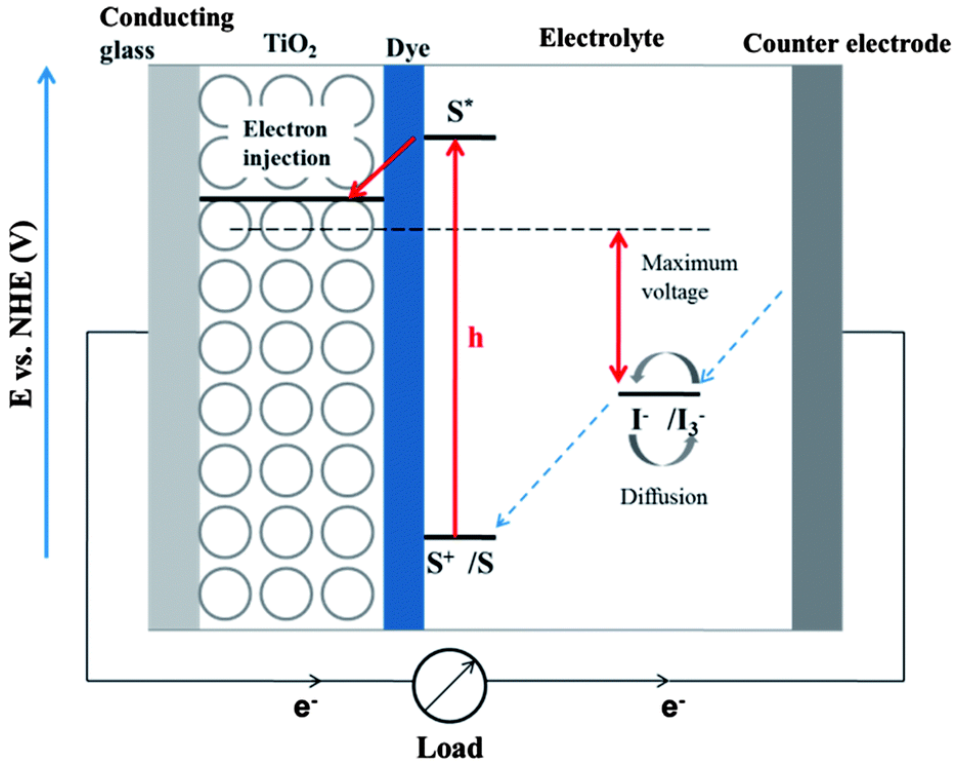

Figure 2: Schematic diagram of a DSSC illustrating the mechanism of electric power generation

Figure 2 shows a schematic of a DSSC describing the mechanism of electricity generation. At first dye, a sensitizer molecule is adsorbed on the surface of a Nano crystalline TiO_2 electrode. Here dye absorbs the incident photon flux and is excited from the ground state (S) to the excited state (S*). One type of photo-excitation causes transfer of an electron from the highest occupied molecular orbital (HOMO) of the sensitizer to its lowest unoccupied molecular orbital (LUMO). Subsequent injection of the excited electron into the conduction band of the TiO_2 electrode results in oxidation of the sensitizer molecule. The injected electron diffuses through the TiO_2 electrode toward the transparent conducting oxide (TCO)-coated electrode and through the external load and wiring, eventually reaches the counter electrode. The oxidized sensitizer is reduced by I^- ions in the electrolyte, regenerating the ground state of the sensitizer, and I^- ions are oxidized to I^{3-} ions [14].Overall, electricity is generated without permanent chemical transformation.

2.3 Advantages of DSSC

Dye-sensitized solar cells have numerous advantages because of their common functionality in low-density applications and portable gadgets. However the first and foremost reason that has made DSSC attractive to worldwide is its low fabrication cost and its eco-friendly nature. There is no possibility of greenhouse gas emission from photovoltaic module since it is produced from organic materials [15]. This organic solar cell is capable of capturing power in low light or even rainy conditions when charge carrier mobility is low and recombination becomes a major issue. Another feature of this solar cell is that it can be made truly transparent color depending on the choice of their sensitizer[16]. The cell do not need large setup for manufacturing, thus it is considerably less expensive compared to the conventional silicon solar cell. DSSC are mechanically robust and can be engineered into flexible, non-fragile, light weight substrates. DSSC panels can also be manufactured in a low-cost process. The production equipment is similar to manufacturing lines used by printing, coating and packaging industries.

2.4Disadvantages of DSSC

The foremost disadvantage of the DSSC design is the use of electrolyte that has temperature stability problems. At low temperature the electrolyte can freeze causing no power production which may lead to potential physical damage. On the other side at high temperature the liquid electrolyte can expand creating problem in the sealing of the panels. The electrolytes are volatile organic compounds (VOC), which must be handled carefully and seal them as they are hazardous to human health and the environment. This along with the fact that the solvent permeate plastics, has precluded large-scale outdoor application. Thus replacement of liquid electrolyte with a solid has been major ongoing field of research [17].

2.5Application of DSSC

Since the DSSC can be flexible it can be employed as promising photovoltaic systems for building integration (BIPV) [18]. It can be transparent with various degrees of transparency that makes it suitable for window applications in building. Also now several companies already started manufacturing DSSC for indoor purposes. For example GCell has introduced flexible

DSSC for indoor and portable application. They have brought cells that can accept indoor lighting system as light sources and their spectral response is similar to human eye [19]. Moreover some portable application includes charger for portable electronics like mobile or camera battery charger ideal for carrying in backpacks [20].

2.6MATERIALS

2.6.1 TRANSPARENT CONDUCTING GLASS

Transparent conductive oxide is a doped metal oxide thin film preferably used in devices such as displays, photovoltaic. During the last thirty to forty years the leading TCOs have been indium oxide (In_2O_3), tin oxide (SnO_2), indium tin oxide (ITO), zinc oxide (ZnO). A TCO is a wide band-gap semiconductor (>3.2eV) that has a relatively high concentration of free electrons in the conduction band which arise either from defects in the material or from extrinsic dopants near the conduction band [21]. The high electron-carrier concentration causes absorption of electromagnetic radiation in both the visible and infrared portions of the spectrum. Till date industry standard TCO is ITO (tin-doped indiumoxide) which has a low resistivity of 10^{-4} Ωcm and a transmittance of greater than 80%[22].In this research work this transparent conduction oxide layer will be used as a substrate for photo anode and counter electrode. Thus the sheet resistance must be independent of calcination temperature 500°C.

2.6.2 PHOTO ANODE MATERIAL

Photoanodes are important components of DSSC because of their functions in supporting dye molecules and transferring electrons. A high electron transport rate is required to reduce electron-hole recombination rate and enhance conversion efficiency. Therefore, a large surface area is necessary to ensure high dye loading. Moreover, a fast charge transport rate is required to ensure high electron collection efficiency.

To produce photo anode TiO_2 paste is coated on ITO glass and then calcinated at 450-500°C. The produced film is porous with about 10μm in thickness because of TiO_2 nanoparticles that has a nano porous structure.Thus high roughness factor of TiO_2 film increases the amount of dye fixed on the surface resulting high light conversion efficiency[23].Also 50-70% porosity of the TiO_2 film can be achieved by adding polymer substrate[24]. In this thesis work polyethylene glycol is used as polymer substrate in the TiO_2 paste solution. In dye-sensitized solar cell dye create a monolayer on TiO_2 surface.

2.6.3 DYE

The absorption of light in the DSSC is achieved through sensitizer embedded in TiO_2 architecture. The sensitizer is comprised of inorganic dye molecules, organic dye molecules and metal–organic dye molecules. The most successful sensitizers in terms of efficiency and stability are based on synthetic dye, but they suffer from several limitations such as higher cost, tendency to undergo degradation and usage of toxic materials. These limitations have opened up for alternate sensitizers that are biocompatible natural sensitizers that contain plant pigments such as anthocyanin, carotenoid, flavonoid, and chlorophyll responsible for chemical reactions such as

absorption of light as well as injection of charges to the conduction band of TiO_2 by thesensitizer[25].Therefore,dyescontainingthesepigmentscaneasilybeextractedfromnaturalproduct slikefruits, flowers, leaves, seeds can be employed as sensitizer for DSSC.

In this research work blackberry dye is employed as sensitizer which has anthocyanin pigment present in it[26]. Anthocyanin is one of the most important group of pigments that are visible to human eye Anthocyanin molecules have carbonyl and hydroxyl groups bound to the surface of TiO_2 semiconductor, which helps in excitation and transfer of electrons from the anthocyanin molecules to the conduction band of porous TiO_2 film [27].

2.6.4 BINDER

The role of binder is to provide the polymeric network that holds the entire chemical system together for further processing. In this research work polyethylene glycol (PEG) is used as the binder. It is utilized as a structural directing agent in thin film fabrication [28]. The presence of binder in an appropriate amount can produce a crack free coating besides improving the strength and density of the electrode after sintering.

2.6.5 ELECTROLYTE

Electrolyte is the hole conducting material. Electrolyte containing I^-/I^{3-} redox ions is used in DSSC to regenerate the oxidized dye molecules. Cell performances are greatly affected by ion conductivity in electrolyte which is directly affected by viscosity of the solvent. Thus solvent with lower viscosity is suggested. The redoxing electrolyte needs to be chosen such that the reduction of I^{3-} ions by injection of electrons is fast and efficient good electronic contact to the dye. However due to evaporation liquid electrolytes hinders fabrication of DSSC since manufacturing requires cells be connected electrically yet separated chemically [29]. Henceforward, a significant shortcoming of liquid electrolyte based DSSC leads to short lifespan.

2.6.6 COUNTER ELECTRODE

In DSSC counter electrode acts as a catalyst for redox couple generation as well as electron collector from the external circuit. The role of counter electrode in DSSC is to reduce I^{3-} to I^- in electrolyte by electrons transferred from photo electrode. The counter electrode should possess two advantages: high catalytic activity and electrical conductivity for achieving high performance. Due to this dual role, counter electrode quickly transport electrons from the electrode substrate to the electrolyte and effectively catalyze the iodide–tri-iodide (I^-/I^{3-}) redox reaction in the electrolyte[30]. The counter electrode also need to be stable as well as have low electrical resistance.

2.7 SUMMARY

In this chapter the state of the art of solar cells and more precisely dye sensitized solar cells are discussed. To understand the operating principle of DDSC its explanation with image is also given. Also descriptive information regarding the commonly used materials and chemicals are brought into this chapter for enhanced knowledge.

Chapter-3: Fabrication of Dye-Sensitized Solar Cell

This chapter describes the fabrication details that are done in laboratory. Section 3.1 informs about the chemicals used for fabricating full DSSC. In section 3.2 apparatus lists are given that are used in the process of formulating cell. Section 3.3 gives the list of major instruments that are necessary in manufacturing. In section 3.4 process of preparing each part of the cell are described in details. After formulating all the parts of the cell, assemble is done and the process is described in section 3.5. Lastly in section 3.6 a short summary is given for this chapter.

3.1 Chemicals

- TiO_2 Powder-Degussa P-25 (USA) (Fig-3c)
- Ethanol (BDH, UK)
- Multi-Wall Carbon Nanotube powder (Fig-3a)
- PEG-800 (Polyethylene Glycol) (Merck, Germany)
- Triton X-100 (Merck, Germany)
- Graphite (Carbon from used Battery) (Fig-3b)
- Citric Acid (Merck, Germany)
- CMC (Merck, Germany)
- Acetyl Acetone (Merck, Germany)
- Distilled water
- Sodium Dodecyl Sulfate (Merck, Germany)

3.2 Apparatus

- Indium doped tin-oxide coated glass substrate (ITO) - Techinstro (L 25mm x W 25mm x T 1.1mm,10Ω/cm^2)
- Indian Blackberry (commonly known as Kalo Jam in Bangladesh)
- Mortar Pastel
- Beaker and Petridis
- Glass rod
- Aluminum Foil
- Tweezers
- Scotch tape
- Binder clips
- Crocodile clips
- Variable Resistor – 10KΩ
- Syringe
- Tissue box

(a)

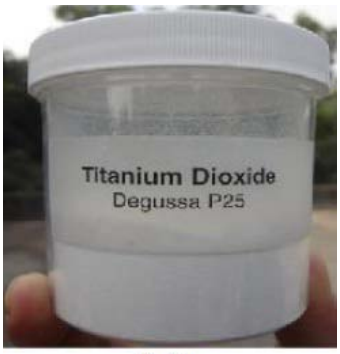

(b)

(d)

(e)

(f)

Figure 3: Images of some chemicals and instruments (a) MWCNT powder; (b) Carbon rod from used battery; (c) TiO2 powder Degussa P25; (d) Weight Machine; (e) Furnace; (f) Probe sonicator

3.3 Instrument

- Probe Sonicator (PCI Analytics Pvt. Ltd., India) (fig-3f)
- Weight Machine (And Gulf, Dubai) (Fig-3d)
- Oven
- Furnace (India) (Fig-3e)
- Multimeter (AGILENT 34401 A)
- Solar Simulator

3.4Preparation Method

Among several coating techniques, Doctor Blade method is applied to coat the ITO glasses for photo anode and counter electrode. It is a promising low-cost method for the preparation of thin films on a wide range of substrates. It is also one of the simplest procedure for ITO coating glasses with paste or suspension formula.

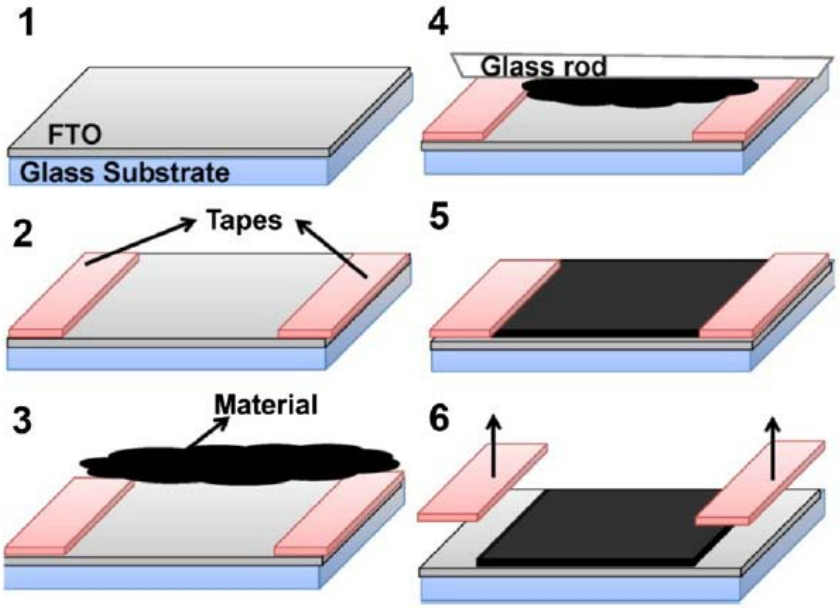

Figure 4: Doctor Blade deposition method step by step in ITO glass substrate using paste or suspension

In this thesis work film coating is done by this method (Fig-4). At first, the thin films are cleaned and tape casted in a table or board maintain 2mm width at the both sides. Now paste substrate is kept in an edge of the glass for filling. For uniform coating in the film glass rod is swept in a rapid motion towards the bottom of the slide and then again in the opposite direction. Without lifting the glass rod same gesture is applied 2/3 times. After deposition of the paste tapes are removed carefully.

3.4.1 Ultrasonic Cleaning of ITO Glass

ITO glass cleaning is the first and one of the most important part of the cell fabrication process. Without proper cleaning the glass cannot be contaminant-free which will have effect on the device performance of the solar cells. Thus now-a-days ultrasonic cleaning method is opted for proper cleaning along with appropriate cleaning solvent. Here ultrasonic cleaning is done by ultrasonic bath sonication which uses high frequency pressure waves to thoroughly clear all

Figure 5: Ultrasonic Cleaning of ITO glasses using cleaning solvent in sonicator

traces of contamination from the surface. At first the ITO glass plates are rinsed with distilled water and then sonicated in Acetone for 15 minutes (Fig-5). After that glass plates are again rinsed with distilled water. Later the ITO substrates are dried at 60°C in oven for few minutes prior to make film.

3.4.2 Preparation of Photo Electrode

Initially the FTO glasses are cleaned with above mentioned process and conductive side is identified measuring the resistivity using multimeter. After that the film is tape casted in a table keeping the conductive part in the upside direction.

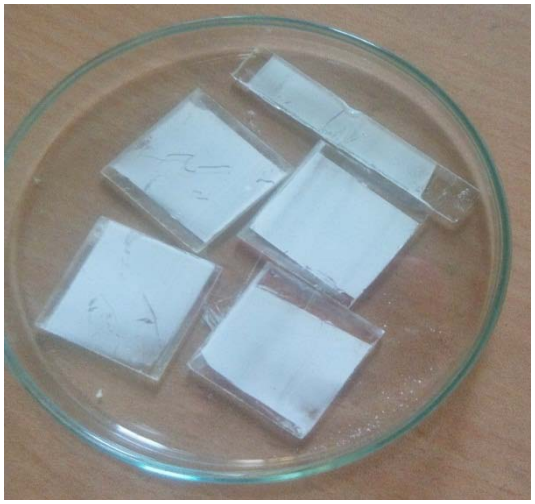

Figure 6: Fully prepared Titanium di-oxide based photo anodes

Now the TiO_2 suspension is prepared by grinding TiO_2 powder mixed with solution. The solution is made up from 1.25mL acetyl acetone, 2.5mL Triton X-100 in distilled water, 5mL PEG in distilled water, 50mL distilled water and mixed in a beaker. To prepare the suspension 3g of TiO_2 powder and 6mL solution are taken in a mortar that has been continuously grinded by pastel until it shows a slurry outcome. After preparing the TiO_2 suspension it is kept in rest for removing bubbles. Finally the TiO_2 suspension is coated on the tap casted ITO glass by doctor blade technique using glass rod. The coated glass then air dried and later on annealed at 450°C for 1h to remove the inorganic substances. The final fabricated photo anode is shown in Fig-6.

3.4.3 PREPARATION OF COUNTER ELECTRODE

In this present work counter electrode modification is done by varying graphite and MWCNT amount ratio in four different ways. The samples are denoted as CE1, CE2, CE3, CE4.

3.4.3.1 PREPARATION OF SAMPLE CE1

The first sample is MWCNT counter electrode which is prepared by the deposition of MWCNT paste on the film using doctor blade method. At first the MWCNT powder is dispersed in water with Carboxyl methyl cellulose (CMC) as binder and surfactant. Thus 30mg of MWCNT is taken with 30mL of Ethanol, 1g Citric Acid and 1g CMC and the mixture is dispersed in probe type ultrasonicator for 1h. The prepared mixture is stored in a tube for future use. Now 10mL of the dispersed mixture is taken to mortar pestle and grinded for 10-15 minutes until most of the ethanol evaporates. When maximum ethanol vaporizes 0.1mL PEG is added to the solution and again grinded till it get paste form.

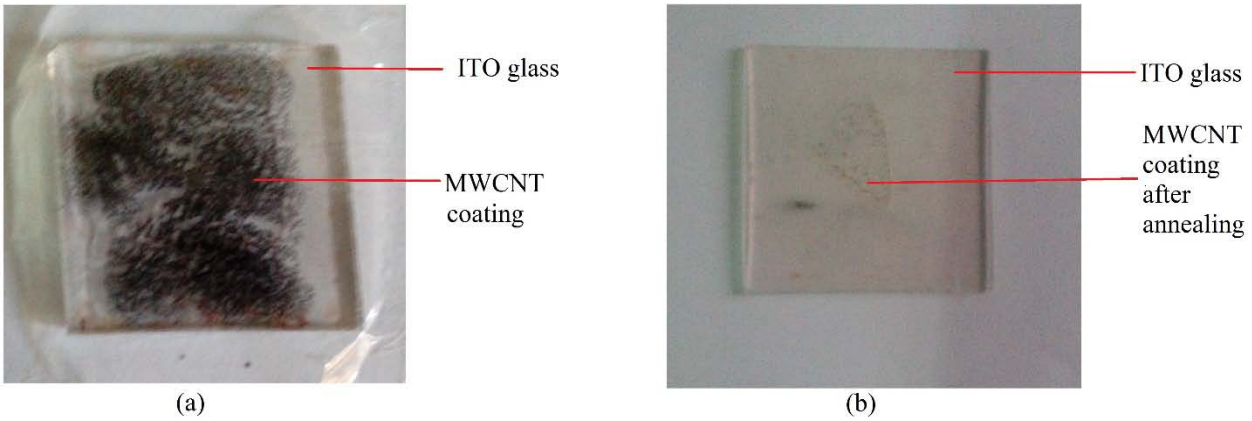

Figure 7: (a) Doctor blade deposition of MWCNT suspension in ITO glass substrate which is kept open for air dried (b) Image of after heat treatment of fabricated MWCNT electrode at 400C for 30 min

Before the deposition process begin the ITO glass is checked for its conductive side by using a mutimeter. Then the glass is tap casted in a table keeping 2mm width from the both side. The formed paste is then coated on the ITO glass using doctor blade technique (Fig-7a). After the deposition in the electrode is done it is allowed to dry in room temperature for several minutes and then heat treated at 400°C for 30 minutes to remove inorganic substrates (Fig-7b).

3.4.3.2 PREPARATION OF SAMPLE CE2

The second sample is graphite based counter electrode where graphite is collected from the old used battery carbon rods (Fig-8a). Since the carbons are in the form of rod, it is crushed in to pieces to get powder form. The crushing is continued for 20 minutes to get small size particles (<20nm).

In a mortar 0.025g graphite powder, 0.06mL distilled water, 0.13mL ethanol and 0.047mL PEG are mixed and grind them with pestle for 10 minutes. 0.06mL distilled water then added each time as the mixture get dried since carbon is hydrophobic and the process is repeated till the mixture become slurry. After the slurry mixture is attained 0.06mL Triton x-100 as surfactant is added to grind them for a minute or two. Since triton x-100 create bubble, the mixture is kept in rest for another few minutes to avoid bubble as it may create crack in the deposition.

Now for the deposition process firstly the conductive side of the ITO glass is identified by multimeter and 2 sides are tape casted keeping 2mm width in a table. Using the formulated paste ITO glass is coated by doctor blade procedure to form a uniform deposition and let it air dried for 30 minutes. Lastly the deposited counter electrode is annealed at 400°C for 30 minutes (Fig-8).

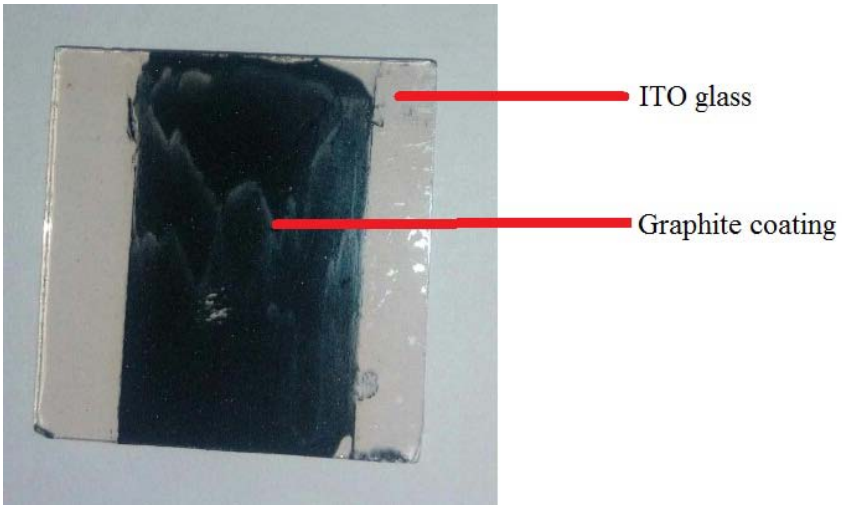

Figure 8: Graphite counter electrode coated by doctor blade technique and annealed at 400C for 30 minutes

3.4.3.3 PREPARATION OF SAMPLE CE3

The third sample is the composite of graphite and MWCNT based counter electrode. For the preparation of this kind of counter electrode paste substrate is needed for coating followed by dorcotr blade technique. Thus total 40mg of graphite and MWCNT mixture (Graphite: MWCNT= 3:1) is added with 0.035g TiO_2, 0.4mL distilled water, 0.4mL ethanol in a mortar. Grinding is done with pestle to get a slurry form for about 10 minutes. Since carbons are hydrophobic in nature the mixture tends to dry out quickly for which 0.4mL water is added and till the mixture becomes slurry water is added repeatedly. The grinding then keeps going for 20 minutes to get a smooth slurry output and 0.18mL Triton X-100 is added after that as surfactant

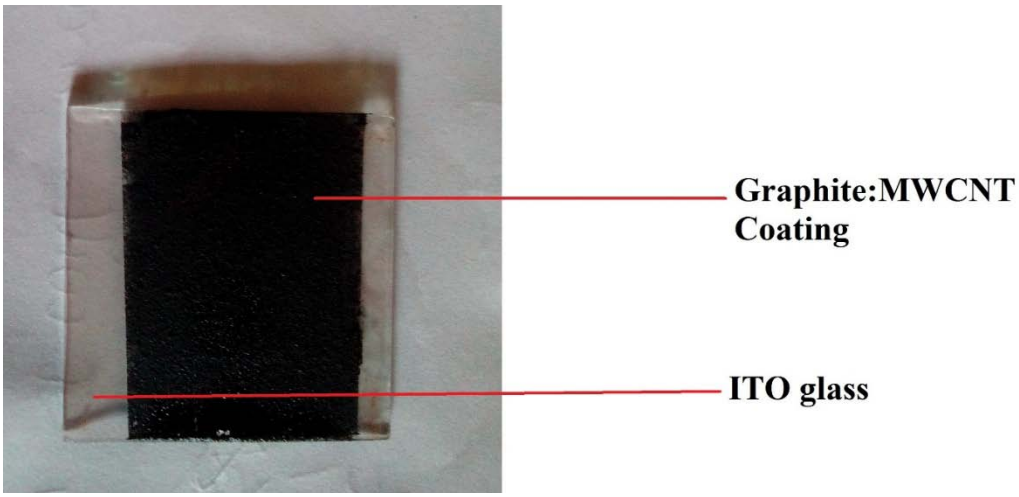

Figure 9: Image of after annealing at 450C for 1 hour of sample CE3 which is Graphite/MWCNT counter Electrode coated by doctor blade method

and grinding get continued for another 2 minutes. The mixture then kept in rest to let the bubble vanish which later will be used to coat ITO glass using doctor blade techniques.

Before deposition conductive side of the ITO glass is identified with the help of multimeter. The film is then tape casted in a table keeping 2mm width of tape from both of the side. The paste substrate is then put in an edge and with the help of a glass rod coating is done following the doctor blade method. After the deposition is done, it is left for air dried for 30 minutes. The electrode is then heat treated at 450°C for 1h in furnace. After the furnace cooled down the glass slide is kept outside (Fig-9).

3.4.3.4 PREPARATION OF SAMPLE CE4

The fourth counter electrode is also a composite of graphite and MWCNT. The preparation of this counter electrode has similarity with sample CE3. However the CE4 counter electrode is the modified version of CE3.

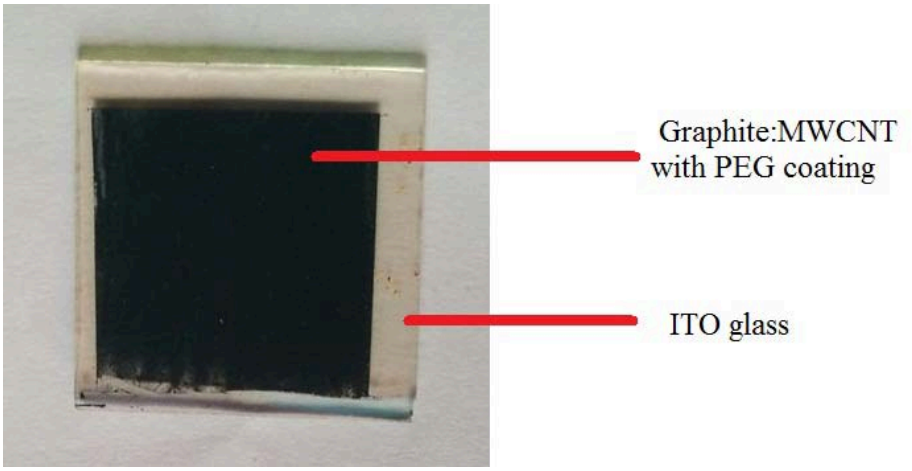

Figure 10: Sample CE4 which is Graphite/MWCNT (with PEG) counter electrode prepared by doctor blade deposition method and annealed at 450C for 1hour

To prepare the sample 0.03g of graphite, 0.01g MWCNT, 0.4mLdistilled water, 0.4mL ethanol, 0.02mL PEG are added in mortar for grinding which will be continued for 20 minutes. When the mixture get dried 0.4mL distilled water is added and the process will be repeated until it get slurry. Here distilled water is added repeatedly because carbon are hydrophobic and the mixture gets dry quickly. After the mixture becomes slurry 0.18mL Triton X-100 is added to the mixture and again grinded for a minute or two. After that the mixture is ready for deposition.

Earlier the deposition is done it is necessary to identify the conductive side of the ITO glass. Thus with the help of multimeter conductive side is recognized and then tape casted in a table keeping the conductive part upside. 2mm width of tape is kept from both of the side. Now the ITO glass is coated using the prepared paste by doctor blade method. The electrode is air dried for 30 minutes and then annealed at 450°C for 1hour in furnace. After the furnace is cooled down the glass slide is kept outside from the furnace (Fig-10).

3.4.4 PREPARATION OF ORGANIC DYE

In DSSC absorption of light is done by dye and in this thesis work Indian Blackberry dye is employed as a natural source of dye. To extract the dye from the Indian Blackberry fruit at first

Figure 11: Blackberry Fruit locally known as Kalojam

the fruits are collected from the local market (Fig-11) and then washed thoroughly removing all sorts of dirt in it. Then the Blackberry is weighted to 5g in digital weight machine and kept in a beaker adding 30mL of solvent. Here solvent can be of methanol, ethanol or propanol. However in this thesis work ethanol is used as solvent for this dye. The Blackberry fruit is soaked in the solvent for 1h storing in a dark space covering with aluminum foil paper. After 1h the extracted dye was filtered with a cotton cloth ensuring purely filtered dye in the beaker.

Now for staining the TiO_2 coated photo anode ITO glass is immersed in dye keeping it for another 1h in a dark place (Fig-12a). It has to be ensured that the film consumes the color of the dye. If white TiO_2 can be seen upon viewing the stained film from either side of the glass slide, then the film should be placed back in the dye for some more times. Later the glass slide is picked up from the immersed solution (Fig-12b) and washed carefully with distilled water. It is important to dry the stained glass slide for removing the water from within the porous TiO_2 film before the iodide electrolyte is applied to the film and thus it is dried in oven at 40°C for 2 minutes. Also it is air dried for another few minutes in a dark place.

3.4.5 Electrolyte

To prepare electrolyte 8.3 g of 0.5 M potassium iodide and 1.27 g of 0.05 M iodine is mixed in ethylene glycol until it is 100 mL. The solution is then stored in an aluminum wrapped bottle and used when necessary.

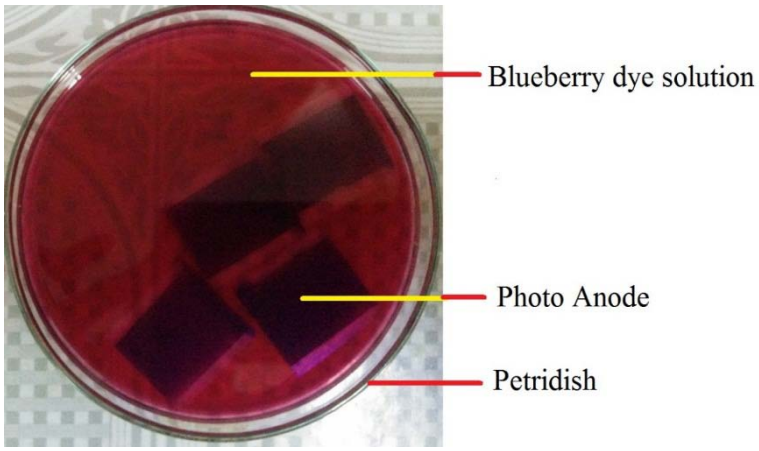

(a)

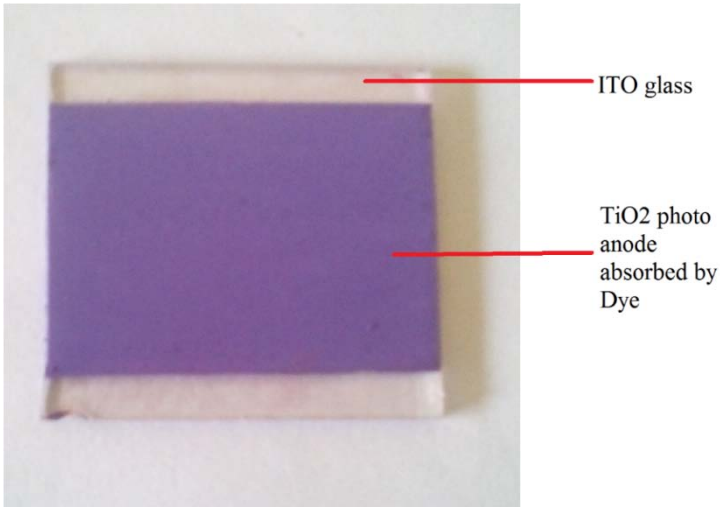

(b)

Figure 12: (a) TiO2 photo electrodes are soaked into the Indian blackberry dye in a Petridis; (b) Blackberry dye absorbed TiO2 photo anode;

3.5 Assemble of Full Cell

To form a full cell to function successfully each of the part are prepared with caution that are described in previous sections. At first photo electrode and photo cathode are placed face to face that the TiO_2 based photo anode and carbon coated counter electrode are in sandwich form and in contact. Two binder clips are used to hold the two longer edges to hold electrodes together. Now 2-3 drops of Iodide electrolyte are injected into the space gap between the electrodes beginning from the one side of the edge. Now the binder clips are alternatively released and returned for distributing the electrolytes evenly on the surface. The liquid electrolytes are drawn into the designated space by capillary action and wet the TiO_2 film. Excess electrolytes from the surrounding areas are then wiped off using cotton swabs and tissues with ethanol. It is very important that the electrolytes from the exposed sides of the cells are removed completely and

precaution should be taken before applying it. Fig-13 represents four types of the full cells prepared in laboratory. Here only counter electrodes are varied.

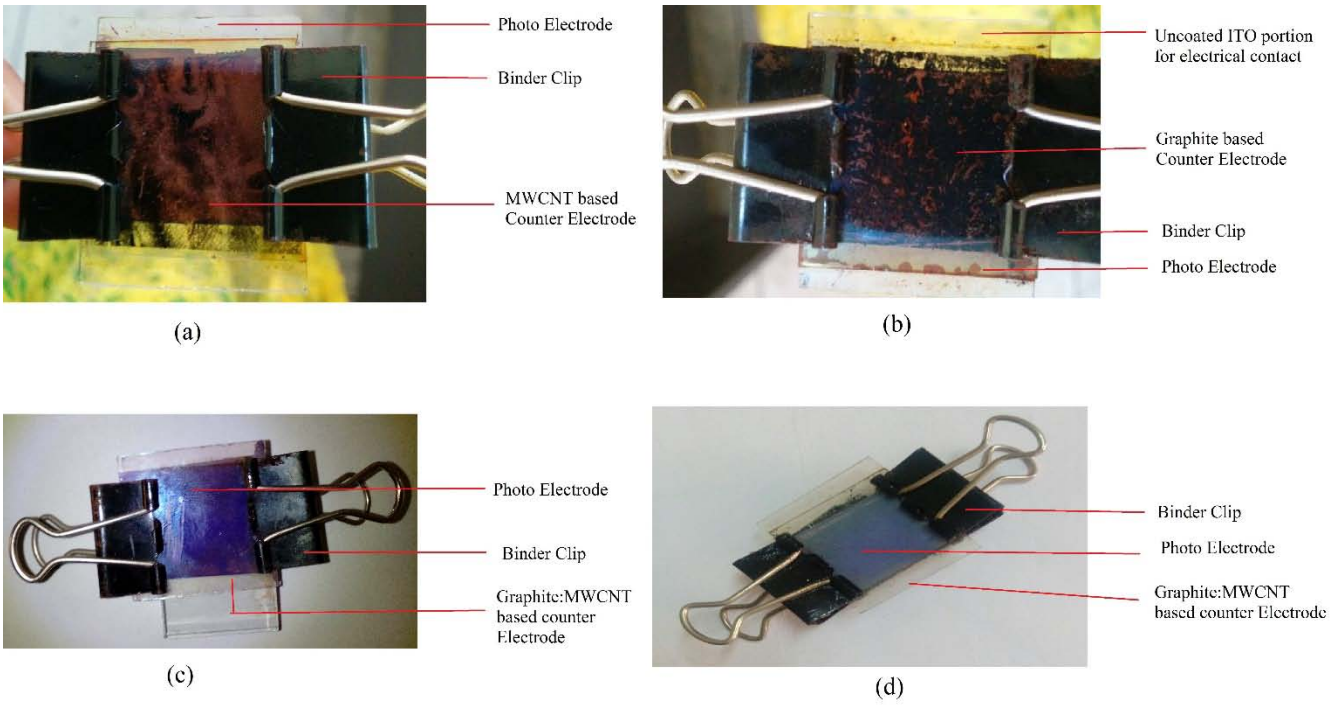

Figure 13: Full assemble of DSSC for testing purpose and four types of counter electrodes are tested (a) Sample CE1 counter electrode made from MWCNT; (b) Sample CE2 counter electrode made from graphite; (c) Sample CE3 counter electrode prepared from graphite:MWCNT ratio of 3:1; (d) Sample CE4 counter electrode prepared from graphite:MWCNT ratio of 3:1

Here Table 1 summarizes preparation procedure of main focus of this thesis which is counter electrode in brief.

Table 1: Sample of counter electrodes and their ratio

Sample Name	Graphite:MWCNT	Annealing Temp.	Annealing Time
CE1	0:1	400°C	30 minutes
CE2	1:0	400°C	30 minutes
CE3	3:1	450°C	1 hour
CE4	3.5:1	450°C	1 hour

3.6 SUMMARY

This chapter completely concentrates on the preparation method and procedure for fabricating four types of counter electrodes, photo electrodes, dye extraction and lastly full cell fabrication. Four different kind of cells are made for characterization and testing purpose which will discussed in chapter four and five consequently.

Chapter-4: Characterization

This chapter purely focuses on the characterization of the fabricated counter electrodes that are described in the previous chapter. Section 4.1 gives a short overview of what characterization is. In section 4.2 Scanning electron microscopy (SEM) images and their analysis are discussed. Section 4.3 provides the transmittance vs. wavelength graphs attained from UV-Visible spectroscopy along with explanations. In section 4.4 electrodes coating thickness information are given examined from microscope. Lastly section 4.5 provides short summary of this chapter.

4.1 Characterization

In the advancement of science and technology the discovery of novel materials are having varied characteristics and their applications are playing an important role. Characterization is an important step in the development of thin film materials. The complete characterization of any material consists of phase analysis, compositional characterization, structural elucidation, micro-structural analysis and surface characterization, which have strong bearing on the properties of materials. In this chapter different analytical instruments will be used to characterize the fabricated films and the findings will be analyzed. Here three different characterizations are done and those are:

Scanning electron microscopy (SEM): Surface roughness study

UV-Visible Spectroscopy: Optical properties study

Microscopic image: Thickness of coating

4.2 Scanning Electron Microscopy (SEM)

SEM analysis is considered to be non-destructive, that is, x-rays generated by electron interactions do not lead to volume loss of the sample, so it is possible to analyze the same materials repeatedly[31]. The signals generated during SEM analysis produce a two-dimensional image and reveal information about the sample including:

- External morphology (texture)
- Chemical composition (when used with EDS)
- Orientation of materials making up the sample

The basic function of SEM is to produce an image of three dimensional appearances derived from the action of an electron beam scanning across the surface of a specimen. The electrons interact with the atoms that make up the sample producing signals that contain information about the sample's surface topography, composition and other properties such as electrical conductivity. Here SEM produce vivid images of sample surface known as secondary electron image (SEI) [32]. In this thesis work the morphological study of the surface of film was done by Scanning Electron Microscope.

4.2.1 SEM ANALYSIS OF SAMPLE CE1

The surface roughness imaging is done with SEM. Before analyzing and capturing the image some parameters are set beforehand which are accelerating voltage, marker and magnifying range. Precise accelerating voltage assures finer image capture which can eliminate unnecessary signals generated from the sample. Here the image of the MWCNT based counter electrode surface is recorded with SEM at 20kv and 1,000 MAG using 10 micron marker.

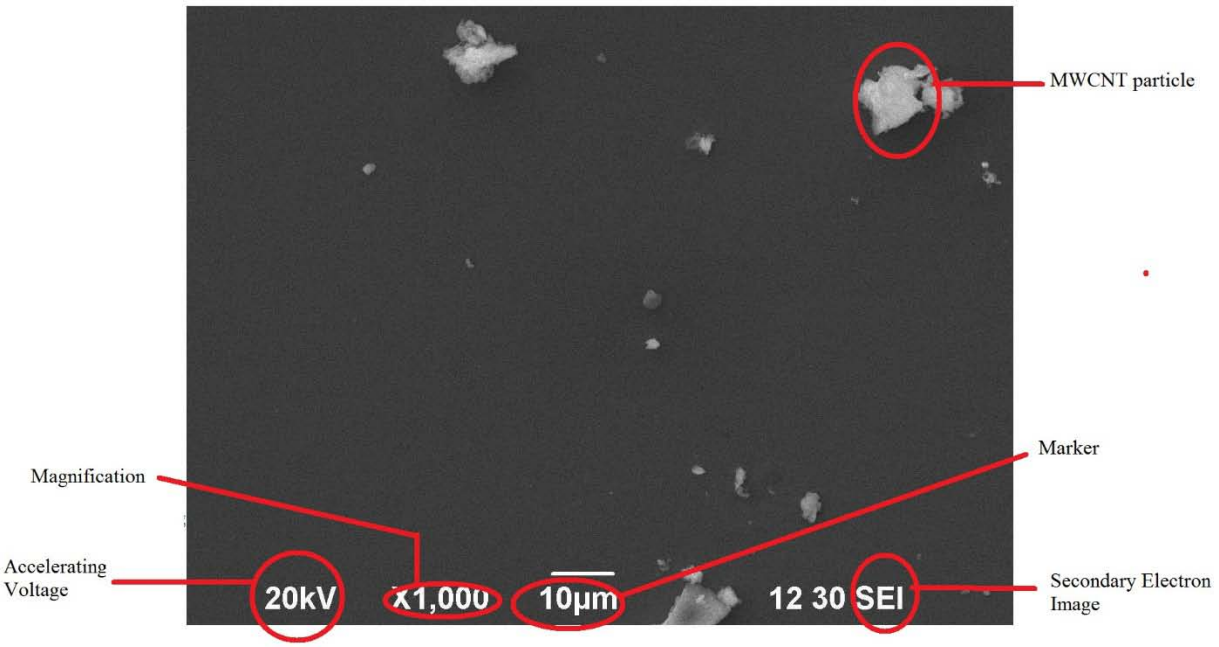

Figure 14: SEM image of MWCNT counter electrode after heat treatment at 400C. SEM image is captured at 20kv and 1,000 MAG using 10 micron marker.

The density of the MWCNT is expressed as the number of MWCNT particles per unit area, which is dependent on the MWCNT concentration within the paste. The image shown in Fig-14 reveals that in this counter electrode MWCNT density is very poor and huge spacing is available between particles. By depositing MWCNTs with large spacing light can pass through the empty spaces providing transparency.

4.2.2 SEM ANALYSIS OF SAMPLE CE2

The surface morphology study of graphite counter electrode is done by SEM. Here SEM produces image which is known as secondary electron image (SEI). The counter electrode surface is recorded at 20kV accelerating voltage and 20,000 MAG using 1 micron marker.In SEM imaging accelerating voltage plays a very important role in capturing impeccable image as finer structure image depends on it. At higher accelerating voltages, the beam penetration and diffusion area become larger, resulting in unnecessary signals generated from the sample. Besides these signals reduce the image contrast and coverS THE fine surface structures.So it is desirable to use low accelerating voltage for observation of low-concentration substances.

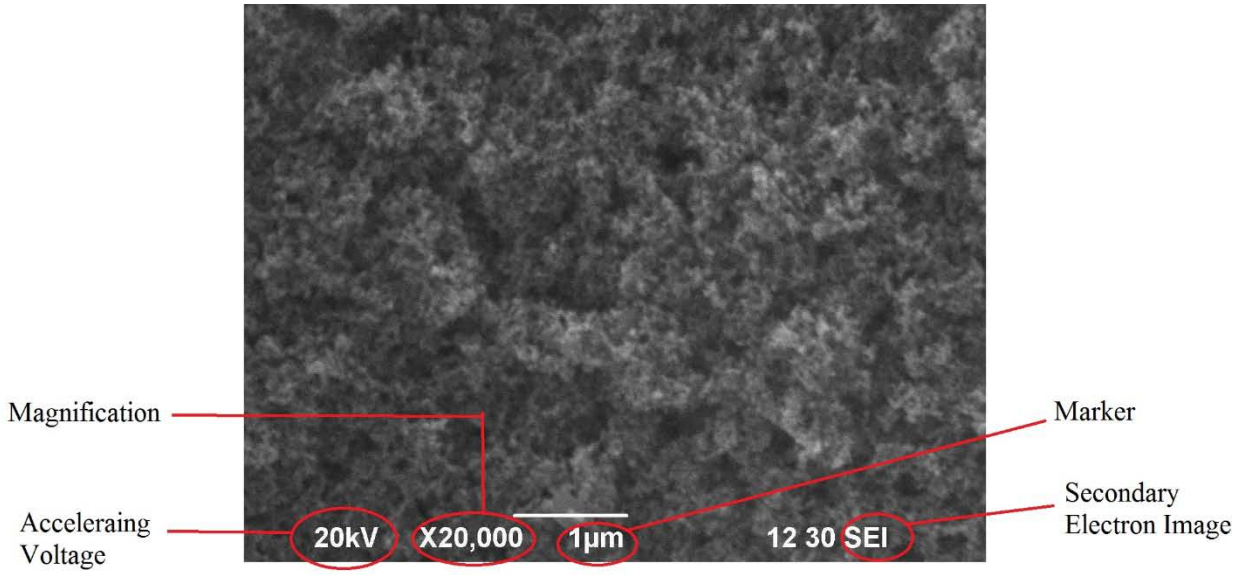

Figure 15: SEM image of graphite counter electrode after heat treatment at 400C. SEM image is captured at 20kv and 20,000 MAG using 1 micron marker.

In this imaging mediocre accelerating voltage 20kV is chosen depending on the sample. In Fig-15 the concentration of the graphite is seen to be highly conjested. Also no spacing is seen between particles which causes the electrode not to trasmit any kind of lights through it. The surface is seen to rough enough causing poor adhesion to the ITO glass substrate.

4.2.3 SEM ANALYSIS OF SAMPLE CE3

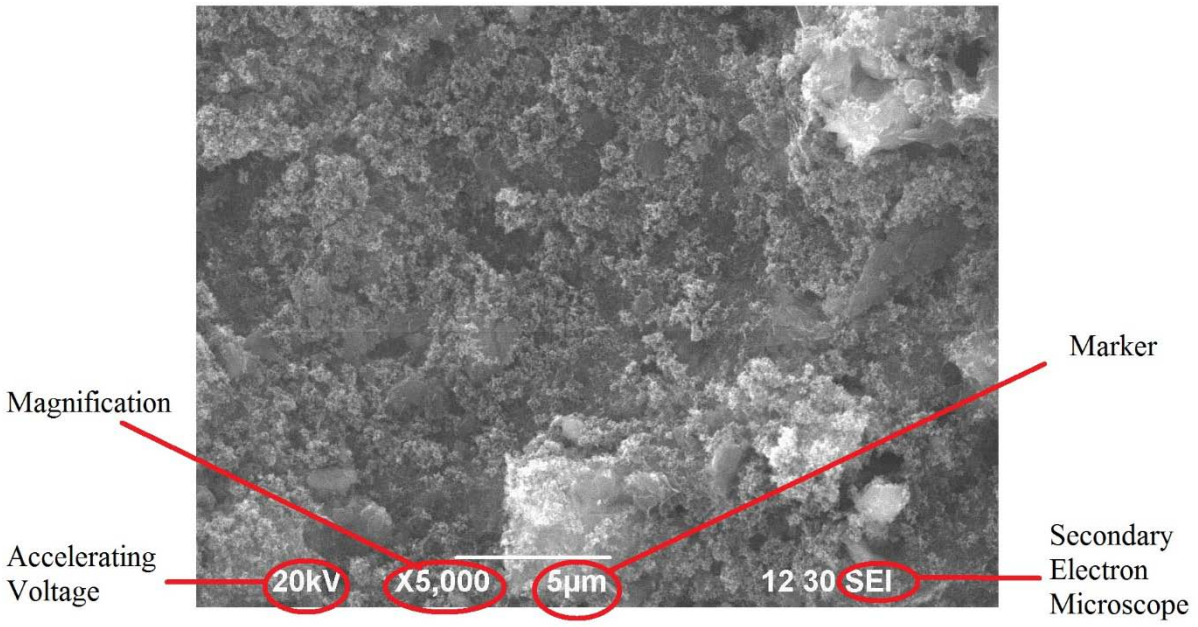

Figure 16: SEM image of Graphite/MWCNT ratio of 3:1 counter electrode after heat treatment at 450C for 1h. SEM image is captured at 20kv and 5,000 MAG using 5 micron marker.

Fig-16 shows the surface morphology of Sample CE3 which is graphite and MWCNT based counter electrode. The counter electrode surface is recorded at 20kV accelerating voltage and 5,000 MAG using 5 micron marker.

The density of a particular substrate is expressed as the number of that substrate per unit area, which is dependent on the substrate particle concentration. The image shown in Fig-19 expresses that in this counter electrode graphite and MWCNT is highly dense. Also some large particles are seen which actually graphite micro particles are. Also from the image it can be seen that the surface is not smooth as expected because of those graphite particles. However the deposition cover large surface area.

4.2.4 SEM ANALYSIS OF SAMPLE CE4

Sample CE4 morphological study is done with SEM which provides vivid image known as secondary electron image. Through this image the morphological condition of that substrate can be studied. Here the image is recorded at 20kV accelerating voltage and 5,000 MAG using 5 micron marker.

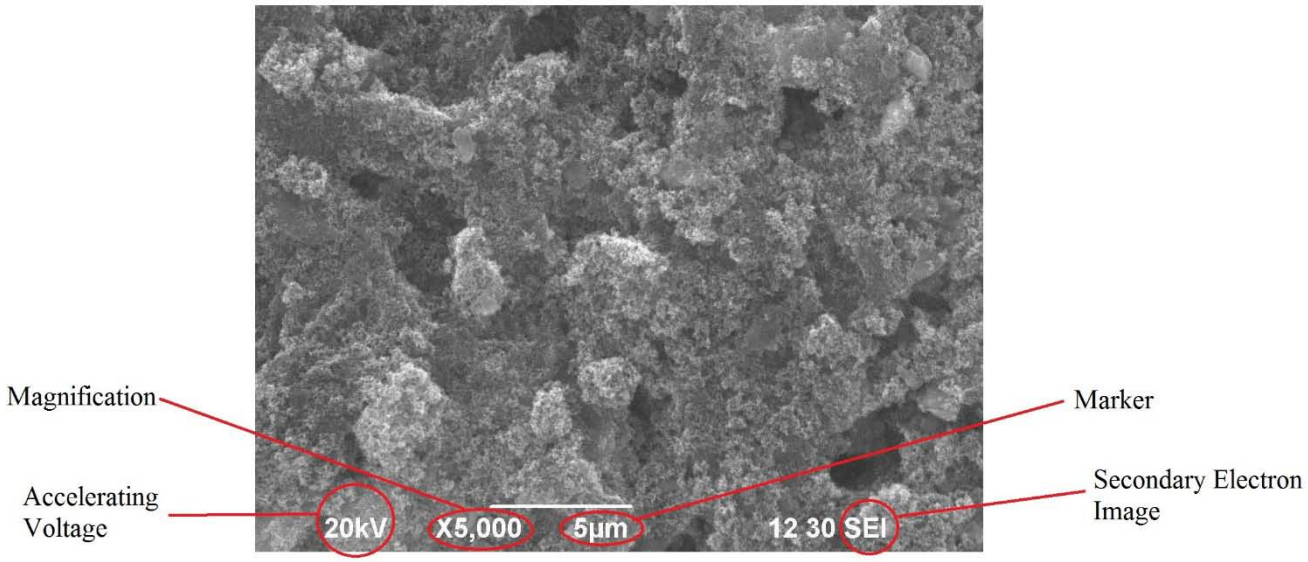

Figure 17: SEM image of Graphite/MWCNT ratio of 3:1 counter electrode with PEG after heat treatment at 450C for 1h. SEM image is captured at 20kv and 5,000 MAG using 5 micron marker.

In Fig-17 it can be seen that the surface area is large and some porous form exists. The porousity is present because of TiO_2 powder. The density is also heavy based on the surface area. Higher density of the particles are caused because of the mixture of graphite and MWCNT powder. Thus it did not show any transperancy like sample CE1. The surface is smooth compared to the sample CE3 as in this electrode PEG is added.

4.3 UV-VISUAL SPECTROSCOPY

Ultraviolet Visible Spectroscopy useful as an analytical technique for two reasons. First it can be used to identify some functional groups in molecules and secondly, it can be used for assaying.

This second role determining the content and strength of a substance which is extremely useful. The optical energy gaps, the allowed direct and indirect transitions and forbidden transitions of optically active substances can be determined from the UV-Visible spectroscopic studies for the potential applications such as light guide material, optical fibers, optical coating to inhibit corrosion etc. The most important application of UV-Visible spectroscopy is to determine the presence, nature and extend of conjugation present in the material.

Figure 18: T60 (PG Instruments) UV-Visible spectrophotometer

In this thesis work optical properties of the counter electrodes are measured with a T60 UV-Visible spectroscopy from PG instruments, U.K. (Fig-18). At first a blank reference cell is kept on the tray of the spectrophotometer and spectrum is taken in transmission operation mode. After that the prepared samples are kept on the tray measuring transmission spectrum with the help of the software.

4.3.1 UV-Visual Spectroscopy Analysis of Sample CE1

The optical absorption of the MWCNT based counter electrode is recorded by UV-visible spectrometer which is shown in Fig-19. The absorption spectra of the counter electrode is ranges from 200-800 nm wavelength. However peak transmittance occurs at 783nm transmitting 120%. At a range of 300nm-400nm the sample presented a low value of transmittance but raised gradually through the visible region. In the visible range which is 400-700 nm the transmittance increases gradually from 81% to 85%, where from 700nm-780nm the transmittance is around 100%. From 780-800nm the transmittance increases to 120%. Thus it can be said that the sample can act as a transparent electrode.

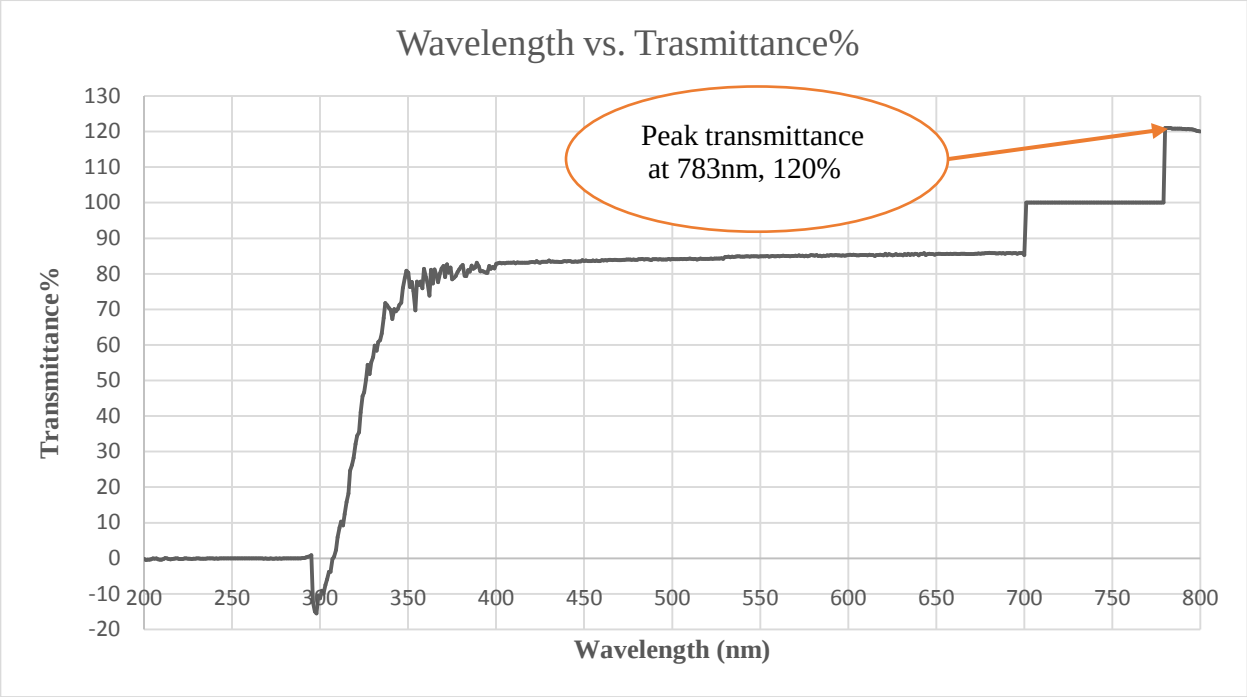

Figure 19: UV-Visible spectroscopy of MWCNT counter electrode (sample CE1)

4.3.2 UV-Visual Spectroscopy Analysis of Sample CE2

Fig-20 shows the representative UV-Visible spectra of sample CE2 which is graphite counter electrode. The transmittance spectra ranges from 200nm-800nm. Here the peak transmittance is shown at 700nm and the transmittance is 3.1% which is very low. The transmittance percentage is very low because it is not transparent rather fully covered with black color. In the visible range which is 400nm-700nm the transmittance shows 0% - 0.1% which means no transmission occurs. This means that in the visible range the counter electrode will not transmit any light.

4.3.3 UV-Visual Spectroscopy Analysis of Sample CE3

The optical absorption spectra of sample CE3 is represented in graph through UV-Vis spectrometer in Fig-21. The spectra ranges from 200nm-800nm which is visible range. In this visible range the transmittance is near 5% which is very low. On the other hand the peak transmittance is seen 56% at 700nm which then drops down gradually to 50%.

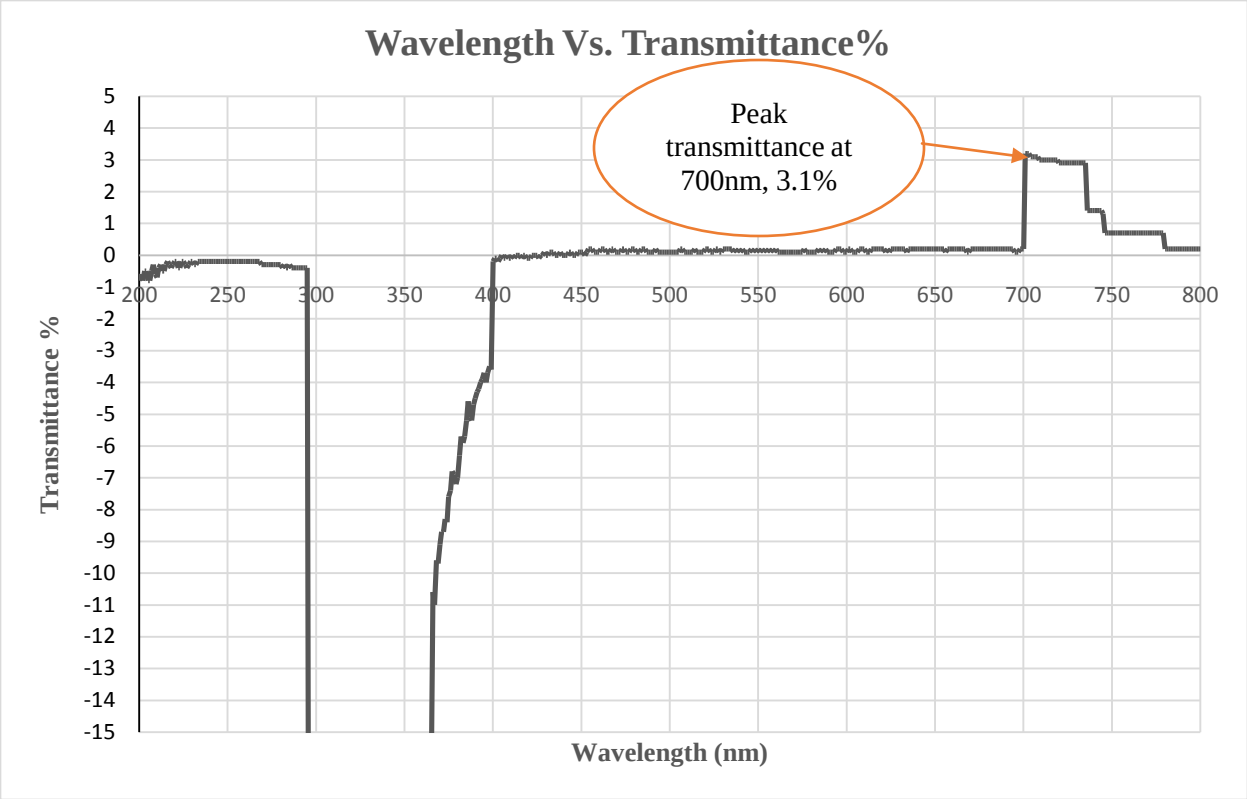

Figure 20: UV-Visible spectroscopy data of sample CE2 - graphite counter electrode

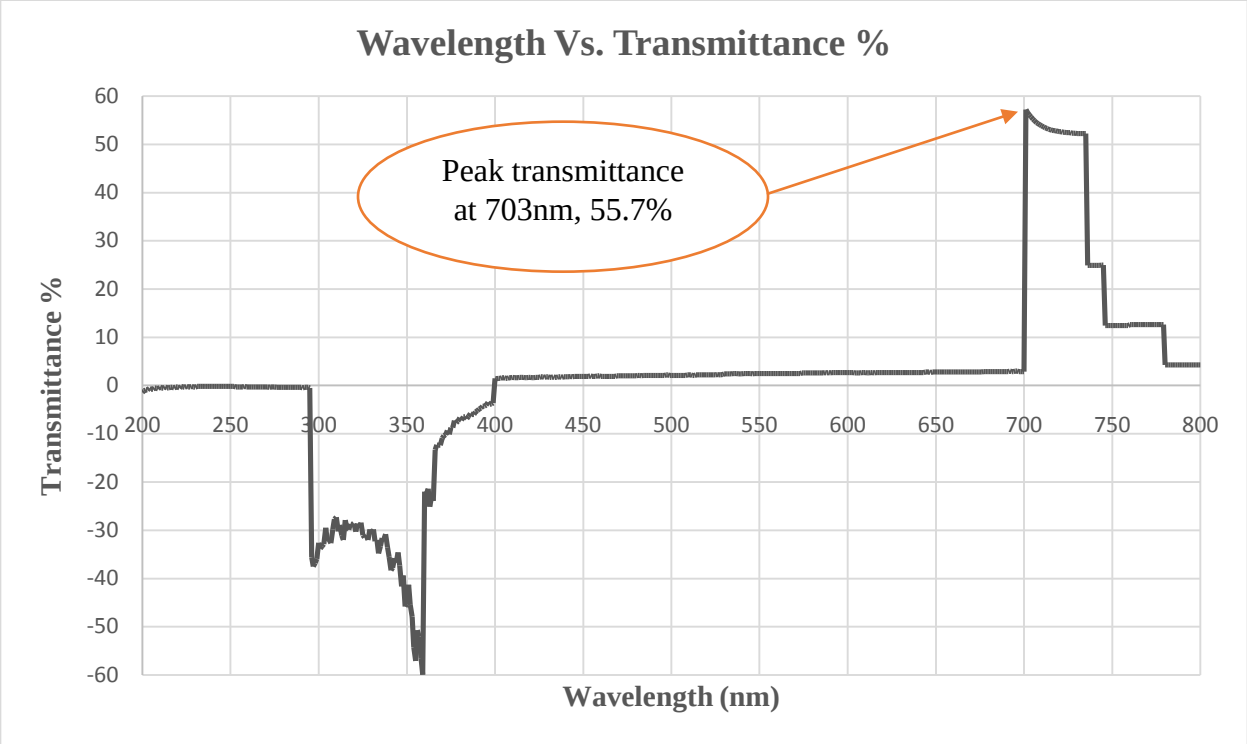

Figure 21: Transmittance analysis of Graphite/MWCNT (without PEG) counter electrode- sample CE3

4.3.4 UV-Visual Spectroscopy Analysis of Sample CE4

In Fig-22 UV-Vis spectra of sample CE4 counter electrode is shown. The spectra is measure by UV-Vis spectrometer ranges from 200nm-800nm. From the image it can be seen that from 200-300nm range the transmittance goes below the negative side which represents reflectance of the electrode. Where on the other hand in visible range which is 400nm-700nm transmittance percentage starts at 5% which gradually increase to 20% at 700nm. A peak transmittance is also seen at 700nm where transmittance is 100%.

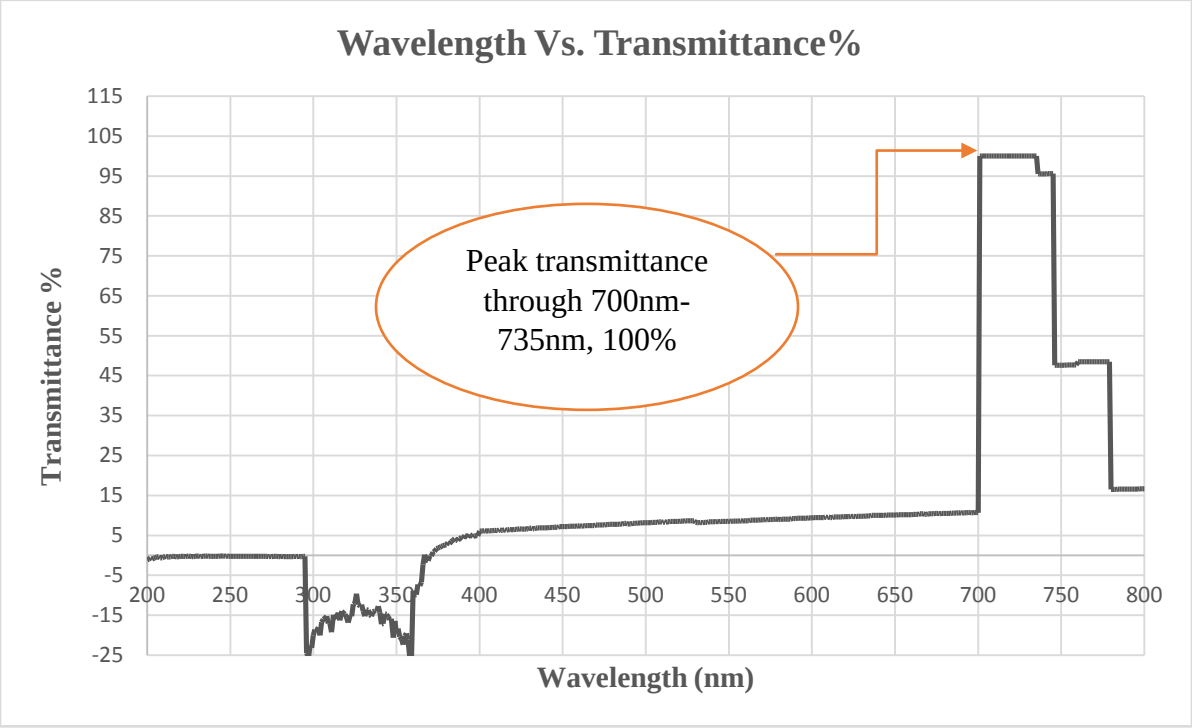

Figure 22: Transmittance vs. Wavelength graph from UV-Visible spectroscopy of Graphite/MWCNT (with PEG) counter electrode (sample CE4)

4.4 Thickness

Another important parameter to look in electrode is the coating thickness. It is found that the cell's overall energy conversion efficiency strongly depends on the electrode with varying thickness. However in this thesis work main focus is given on material not coating thickness. Thus with the help of microscope only coating thickness measured.

4.4.1 Thickness of Sample CE1

From Fig-23 it can be seen that the coating thickness measured is 7.895 micron. Microscope at first capture one portion of the electrode and then with the help of image analysis software provided with the microscope the thickness is calculated.

According to Seung et. al. for transparent CNT electrode minimum 5µm thickness is required and here 7.895µm thickness is found which is quite close.

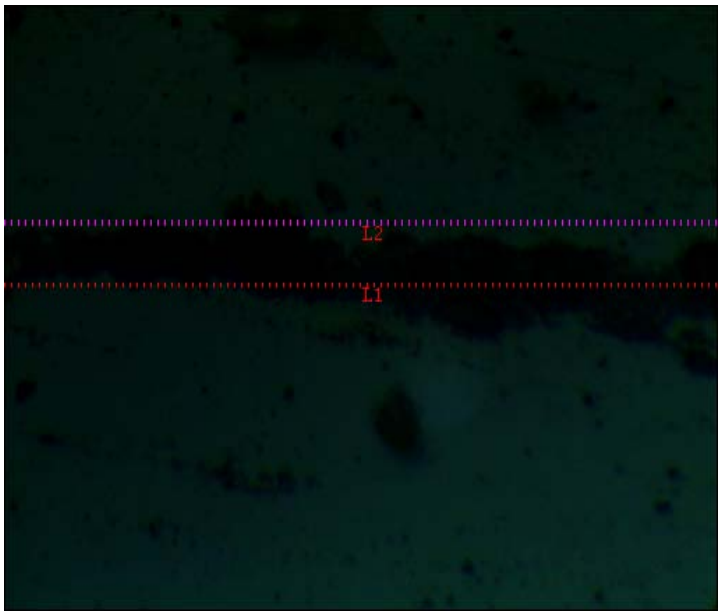

Figure 23: Deposition thickness of MWCNT counter electrode. Thickness is 7.895 micron.

4.4.2 Thickness of Sample CE2

Fig-24 represents the coating thickness of sample CE2 which is graphite based counter electrode. The thickness is measured by first capturing a side image with microscope and then with image analysis software provided with the instrument. The software has some other measurement features. However here only thickness measurement feature is needed. The software measure 15.785 micron as thickness of the coating.

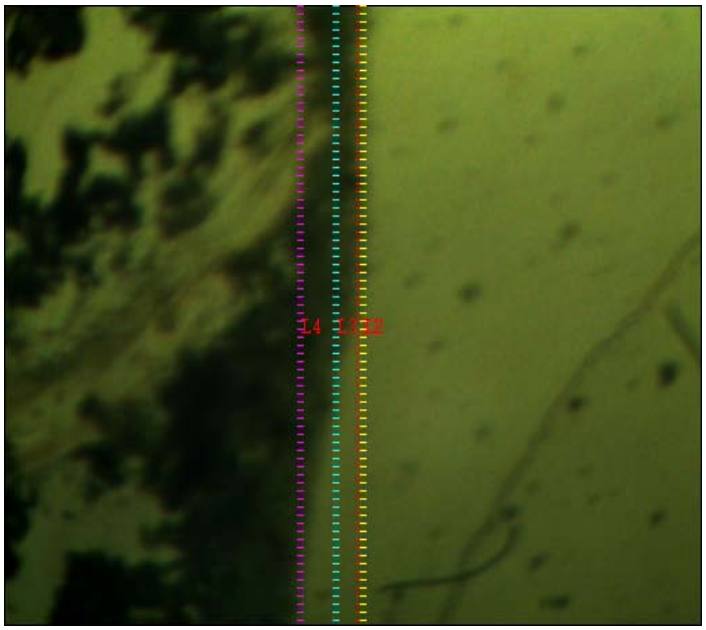

Figure 24: Deposition thickness of Graphite counter electrode. Thickness is measured by microscope. Thickness is 15.785 micron.

4.4.3 Thickness of Sample CE3

The sample CE3 coating thickness is measured from the microscopic image captured by the microscope (Fig-25). The thickness is measured 5.263 micron.

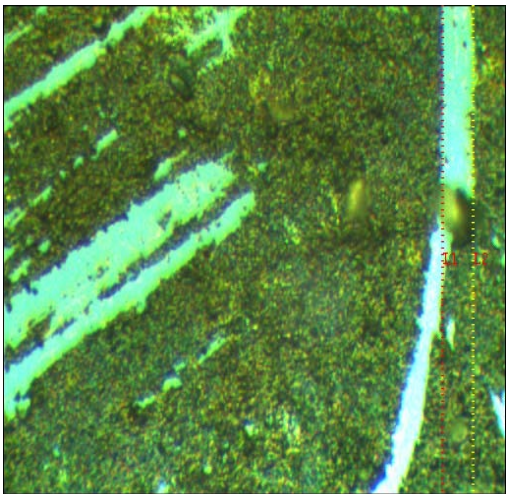

Figure 25: Thickness measurement of Graphite/MWCNT counter electrode through microscopic image. Here the deposition thickness is 5.263 micron.

4.4.4 Thickness of Sample CE4

Fig-26 represents the coating thickness of sample CE4 which is graphite and MWCNT based counter electrode. The thickness is measured by capturing a edge of the slide with microscope and

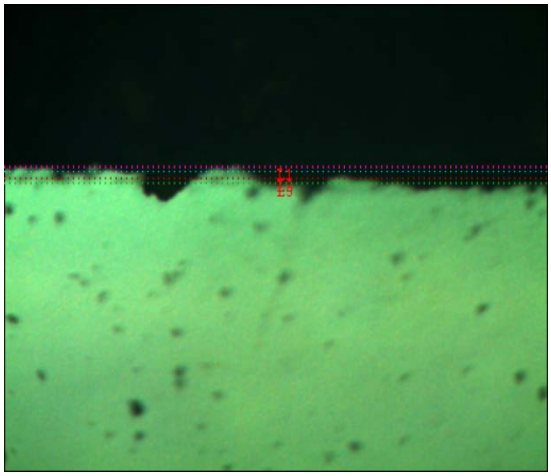

Figure 26: Deposition thickness of Graphite/MWCNT (With PEG) counter electrode. Here, the thickness is 5.263 micron.

then with the help of image analysis software the thickness is calculated. Here the coating thickness is 5.263 micron.

4.5 SUMMARY

This chapter elaborates the description of instruments and methods that are used to prepare and characterize the samples. The experimental procedures and theories have also been discussed in this chapter. The experimental design of this research work involves the preparation of the sample and then characterized by scanning electron microscope (SEM), UV-Visible spectroscopy (UV-Vis), and microscope for deposition thickness which are also discussed on their designated sections.

Chapter-5: Results &Discussions

The chapter concentrates on the findings derived from the I-V and P-V curves of the prepared cells. In section 5.1 short overview of the photovoltaic parameters are given. Section 5.2 describes the experimental setup required for testing and section 5.3 explains the procedure for measuring voltage and current. In section 5.4 detailed analysis of the I-V and P-V curves of the prepared cells are discussed. Section 5.5 comprises of the comparison of the fabricated cells. In section 5.6 discussion upon the result obtained are given. Section 5.7 gives a short summary of this chapter.

5.1 Photovoltaic Parameter

The main parameters that are used to characterize the performance of solar cells are the maximum power P_{max}, the short circuit current I_{sc}, the open circuit voltage V_{OC} and the fill factor (FF). These parameters are determined from the illuminated I-V characteristic. The photoelectric conversion efficiency η can be determined from these parameters.

5.1.1 Open Circuit Voltage, V_{OC}

Open-circuit voltage (V_{OC}) is the maximum voltage a solar cell can provide to an external circuit, which is derived from the splitting of hole and electron quasi-Fermi levels[33]. The open-circuit voltage corresponds to the amount of forward bias on the solar cell due to the bias of the solar cell junction with the light-generated current. An equation for V_{OC} is found by setting the net current equal to zero in the solar cell equation to give:

$$Voc = \frac{kT}{q}\ln\left(\frac{I_L}{I_o} + 1\right) \approx \frac{kT}{q}\ln\left(\frac{I_L}{I_o}\right)$$

Here the approximation is justified because $I_L >> I_o$

The above equation shows that V_{OC} depends on the saturation current of the solar cell and the light-generated current. While Isc typically has a small variation, the key effect is the saturation current, since this may vary by orders of magnitude. The saturation current, I_O depends on recombination in the solar cell. Open-circuit voltage is then a measure of the amount of recombination in the device .

5.1.2 Short Circuit Current, I_{SC}

The short-circuit current is the current through the solar cell when the voltage across the solar cell is zero which means the solar cell is short circuited. The short-circuit current is due to the generation and collection of light-generated carriers. For an ideal solar cell at most moderate

resistive loss mechanisms, the short-circuit current and the light-generated current are identical. Therefore, the short-circuit current is the largest current which may be drawn from the solar cell.

5.1.3 Fill Factor, FF

The Fill Factor (FF) is essentially a measure of quality of the solar cell. It is calculated by comparing the maximum power (P_{max}) to the theoretical power (P_T) that would be output at both the open circuit voltage and short circuit current together. FF can also be interpreted graphically as the ratio of the rectangular areas depicted in Figure 13.

$$FF = \frac{P_{max}}{P_T} = \frac{J_{max} V_{max}}{J_{sc} V_{oc}}$$

5.1.4Conversion Efficiency, η

The conversion efficiency is calculated as the ratio between the maximal generated power and the incident power. As mentioned above, solar cells are measured under the STC (AM1.5, irradiance= 100W/cm^2, temperature=300K).

$$\eta = \frac{P_{max}}{P_{in}} = \frac{V_{OC} I_{SC} FF}{P_{in}}$$

P_{in} is taken as the product of the irradiance of the incident light, measured in W/m^2 or in suns (1000 W/m^2 or 100mW/cm^2), with the surface area of the solar cell [m^2 or cm^2].

5.1.5 I-V measurement

IV measurements constitute the basic solar cell characterization method which is important to determine the key performance parameters. The short circuit current density (J_{sc}), open circuit voltage (V_{OC}), fill factor (FF) and the cell efficiency (η) are the fundamental characterization parameters which can be obtained through current–voltage (IV) curve of the solar cell (Figure 27). The IV curves are normally recorded with a solar simulator in an artificial light intensity of 1000 W/m^2 which is equivalent to 1 Sun light intensity.

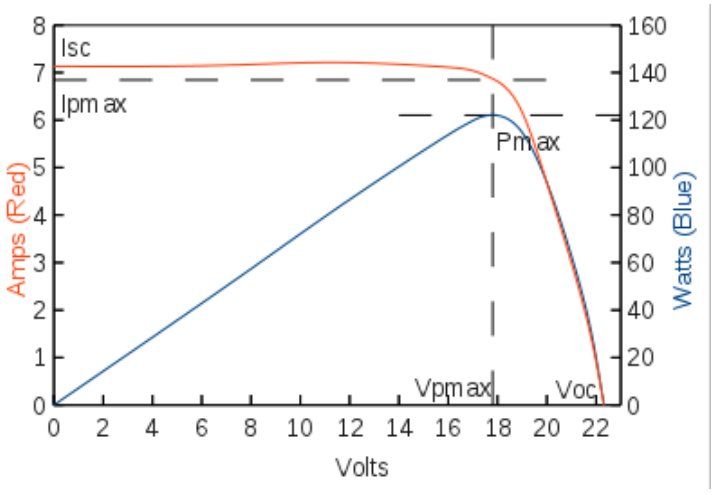

Figure 27: Ideal I-V Curve of solar cell

Referring to figure 27, the span of the I-V curve ranges from the short circuit current (Isc) at zero volts, to zero current at the open circuit voltage (Voc). At the 'knee' of a normal I-V curve is the maximum power point (Imp, Vmp), the point at which the cell generates maximum electrical power.

5.2 Experimental Setup

The completed solar cell is now taken inside a solar simulator under illumination of 100 W/cm^2. The lamp almost imitates spectrum of sunlight. The cell performance was measured using AGILENT 34401A precision multimeter. The testing temperature was 25 ^{0}C to 29 ^{0}C. Maximum voltage, current and resistance were determined by attached a multimeter directly to the two sides of the cell using wires with crocodile clips (Fig-28).

The negative electrode is the TiO_2 coated glass that was attached to the black (-) probe of the meter and the red (+) probe was to the counter electrode.

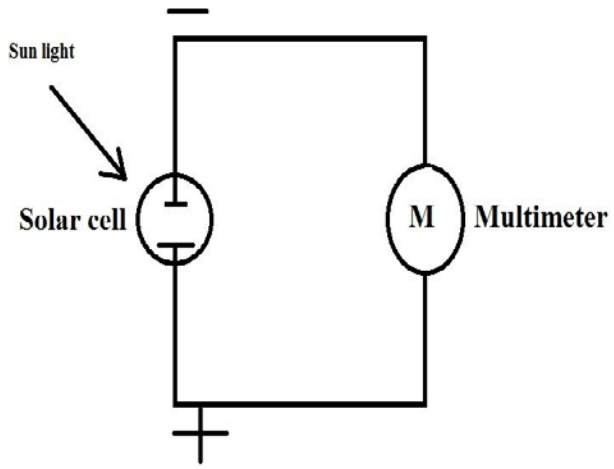

Figure 28: Schematic diagram of experimental setup to measure open circuit voltage (Voc) and short circuit current (Isc)

5.3 Measurement of Voltage, Current

To test the voltage of the prepared cells, a multimeter is connected in parallel with them.The negative probe was placed on theTiO_2coated photo anode slide and the positive probe on the counter electrode slide.

The open circuit voltage is measured by connecting the solar cell parallel to the multimeter. Meter was set to dc volts and determines the open circuit voltage (V_{OC}).

The short circuit current is also measured similarly. However multimeter is changed to mA from V and the negative pole of the meter is moved to current point.

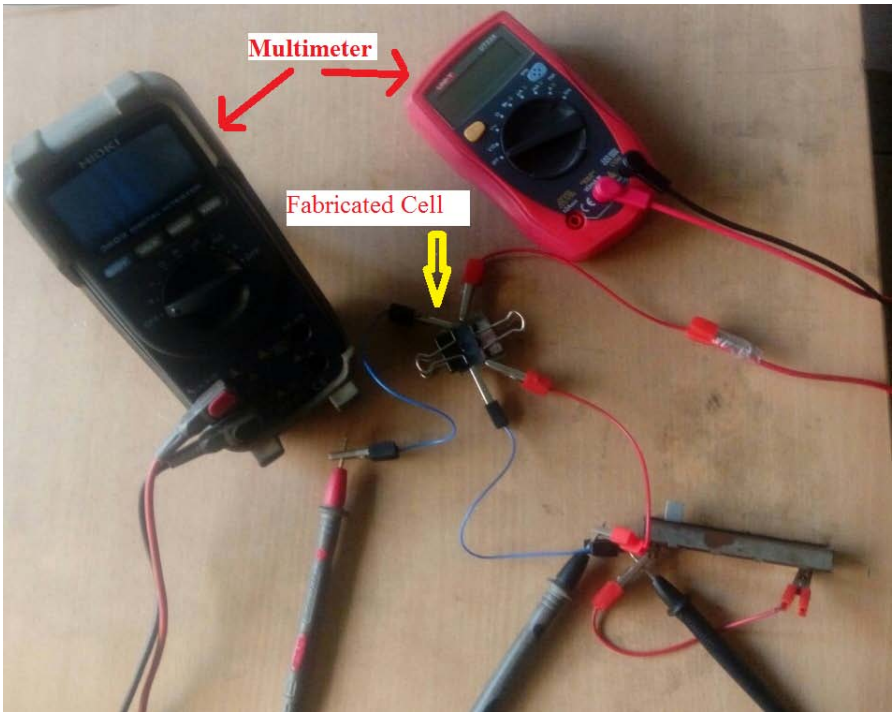

Figure 29: Schematic diagram to measure current and voltage for different load condition

Now to plot IV curve and PV curve current and voltage readings are required for each of the samples. Thus to get the reading experimental setup is constructed as figure. Here, the developed solar cell is working as a source and a variable resistor as load is connected in series. To measure the provided current of the cell multimeter is attached in series of the cell. On the other hand another multimeter is connected in parallel with the cell to measure the voltage. Now resistor is varied and current and voltage reading is collected (Fig-29).

5.4 Sample Analysis

To characterize the performance of the developed solar cells based on the variation of counter electrodes, I-V and P-V curves are plotted and comprehensively analyzed for their fill factor and efficiency.

Fill factor is a parameter that reflects the maximum power output from the solar cell device. As for dye-sensitized solar cells, the practical fill factor is usually lower than the maximum possible one due to the presence of parasitic resistive losses and the charge recombination at semiconductor/redox electrolyte interface. The impact of parasitic resistances depends on the geometry of the solar cell. The most common parasitic resistances are series resistance and shunt resistance. The series resistance reduces the fill factor and thus the efficiency of solar cell by dissipating power in the resistances. The origination of series resistance may be from 1) the movement of electrons through porous structured semiconductor and the diffusion of ions through the electrolyte, 2) the contact resistance at the interface between the semiconductor and the transparent conductive film, and 3) the resistance of the top and rear metal contacts.

The shunt resistance is typically due to the manufacturing defects, which cause power losses in solar cell by providing an alternate current pathway for the photogenerated carriers. In general, a small series resistance and a large parallel resistance are thought to be beneficial to achieving a high fill factor.

The Figure 32 illustrates the shift in I-V curve due to internal resistance and corresponding shifts in Voc, Isc and Fill Factor (FF).

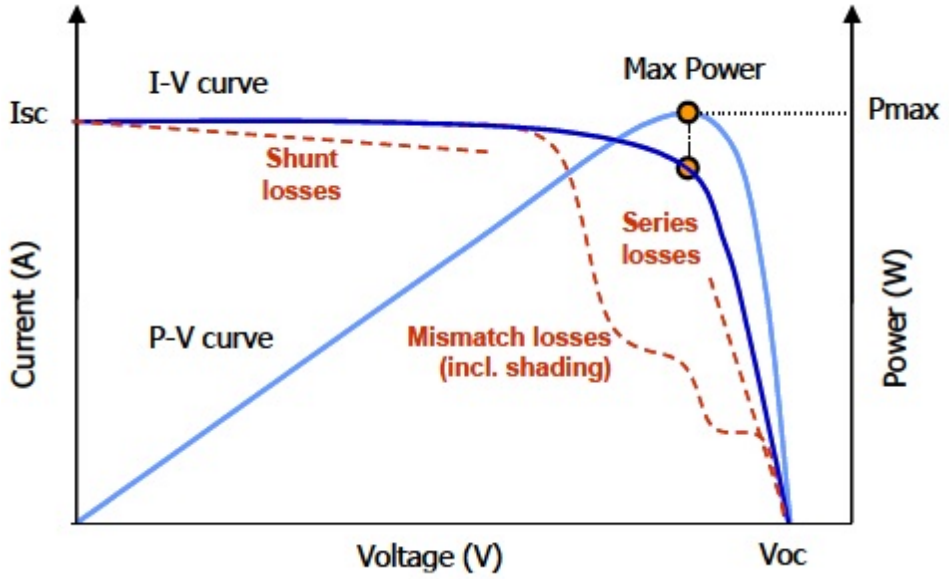

Figure 30: Several categories of losses that can reduce PV array output. The I-V curve provides important troubleshooting clues.

Any impairment that reduces the fill factor also reduces the output power by reducing Imp or Vmp or both. The I-V curve itself helps to identify the nature of these impairments. The effects of series losses, shunt losses and mismatch losses on the I-V curve are represented in Figure 30.

5.4.1 Sample CE1 Analysis

Figure 31 shows the I-V characteristics of a DSSC operating under normal conditions. The power delivered by a solar cell is the product of current and voltage (I x V). If the multiplication is done, point for point, for all voltages from short-circuit to open-circuit conditions, the power curve above is obtained for a given radiation level.

With the solar cell open-circuited, that is no load, the current will be at its minimum (zero) and the voltage across the cell is at its maximum, known as the solar cells open circuit voltage, or Voc. For this sample the open circuit voltage is 450mV. On the other hand, when the solar cell is short circuited, that is the positive and negative leads connected together, the voltage across the cell is at its minimum (zero) but the current flowing out of the cell reaches its maximum, known as the solar cells short circuit current, or Isc. Here the short circuit current is 0.334mA.

However, there is one particular combination of current and voltage for which the power reaches its maximum value, at Imp and Vmp. In other words, the point at which the cell generates

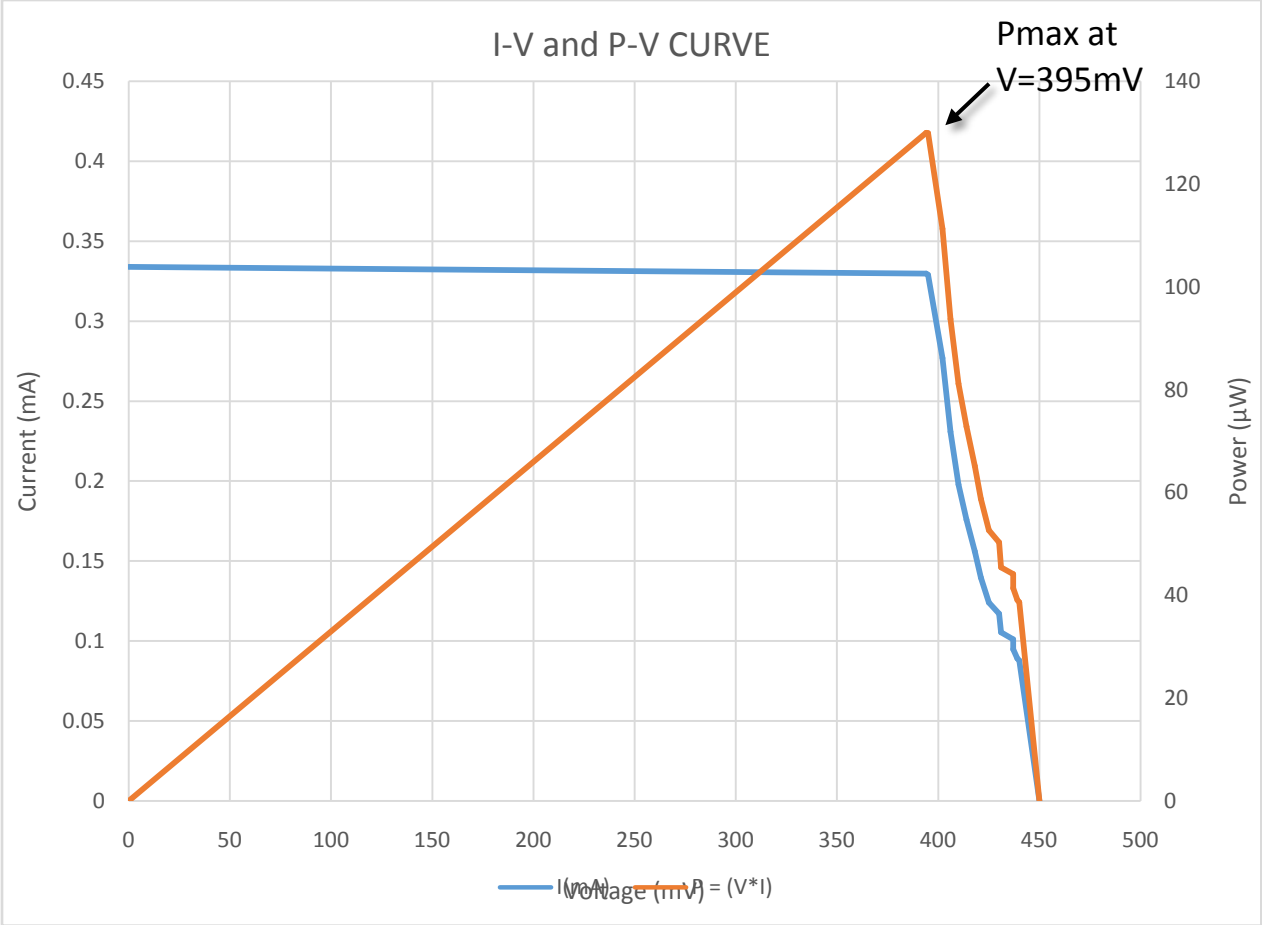

Figure 31: I-V and P-V curves of sample CE1 counter electrode. The counter electrode is prepared from Multi Wall Carbon Nanotube using Doctor Blade Technique.

maximum electrical power which is the "maximum power point" or MPP. From figure 31, the maximum power for this particular sample is 129.955µW. Therefore the ideal operation of a photovoltaic cell is defined to be at the maximum power point. The maximum power point (MPP) of a solar cell is positioned near the bend in the I-V characteristics curve.

Now by analyzing figure 31 which represents the I-V curve of sample CE1 for fill factor it can be seen that some internal series losses exists. However the fill factor is quite notable considering other data from table 2.

5.4.2 Sample CE2 Analysis

A solar cell produces its maximum current when there is no resistance in the circuit. This maximum current is known as the Short Circuit Current, Isc and in this developed cell the Isc is 0.146mA.

Conversely, the maximum voltage occurs when there is a break in the circuit. This is called the Open Circuit Voltage (Voc). Under this condition, the resistance is infinitely high and there is no current, since the circuit is incomplete. In this sample the Voc is 30mV from figure 32.

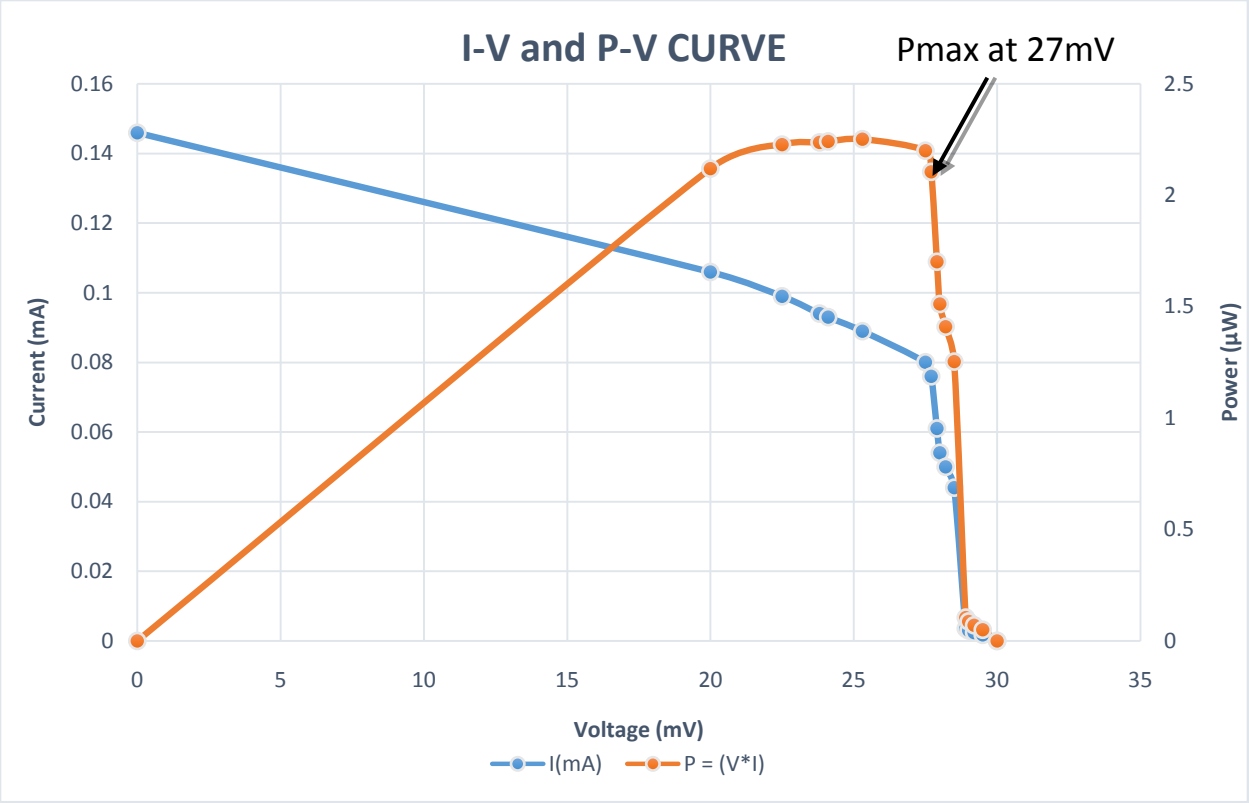

Figure 32: I-V and P-V characterization of CE2 sample. Here the counter electrode is made from graphite only using doctor blade deposition technique

There is a point on the knee of the I-V Curve where the maximum power output is located and this point is called the Maximum Power Point (MPP). The voltage and current at this Maximum Power Point are designated as Vmp and Imp. Here Vmp=27mV and Imp=0.076mA. Thus Pmax= 2.1052µW from figure 32.

Figure 32 depicts graphical representation of I-V of sample CE2. The counter electrode of this sample is prepared from graphite. The figure shows that there is some internal shunt losses exist in the cell which causes the curve to fall sharply from the short circuit current. Since shunt loss occurs because of manufacturing defect, it can be assumed that size of the graphite particles may be the one of the root causes.

5.4.3 Sample CE3 Analysis

The open circuit voltage for this CE3 sample is 567mV and short circuit current is 0.1836mA.

There is a point on the knee of the I-V Curve where the maximum power output is located and this point is called the Maximum Power Point (MPP). The voltage and current at this Maximum Power Point are designated as Vmp and Imp. Here Vmp=450mV and Imp=0.1mA. Thus Pmax= 43.8µW (Fig33).

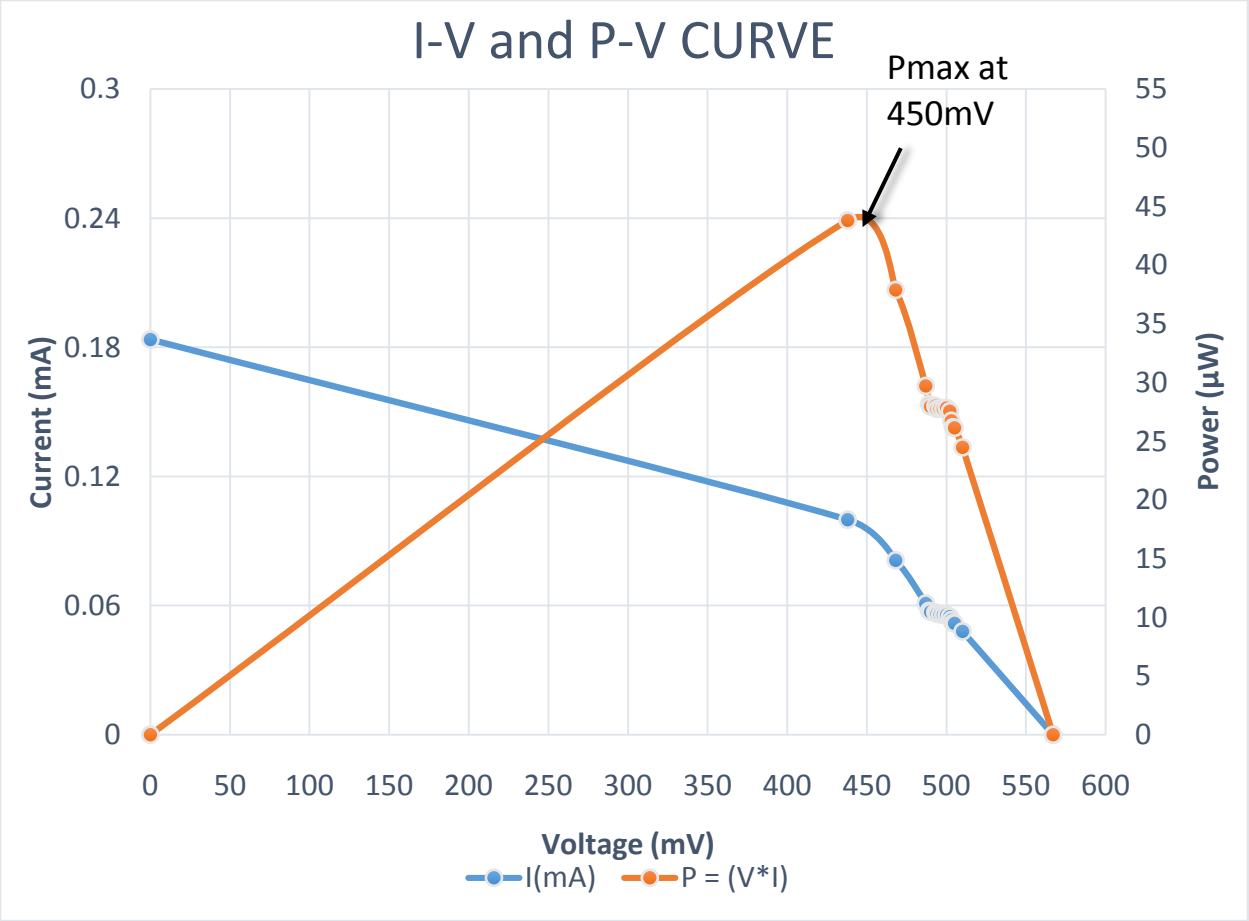

Figure 33: I-V and P-V curves of sample CE3. The cell counter electrode is prepared from graphite/MWCNT composite material

I-V curve of sample CE3 can be seen from figure 33. The calculation of the fill factor shows quite low in consideration with the reference electrode which is platinum. The graph also depicts that it has some shunt and series loss internally.

5.4.4 Sample CE4 Analysis

Drawing the curve, there is only one point where at which maximum power (Pm), expressed in watts of the solar cell is delivered. This break point is known as maximum power point (MPP). In this sample the MPPT point is 332.7µW (Fig-34).

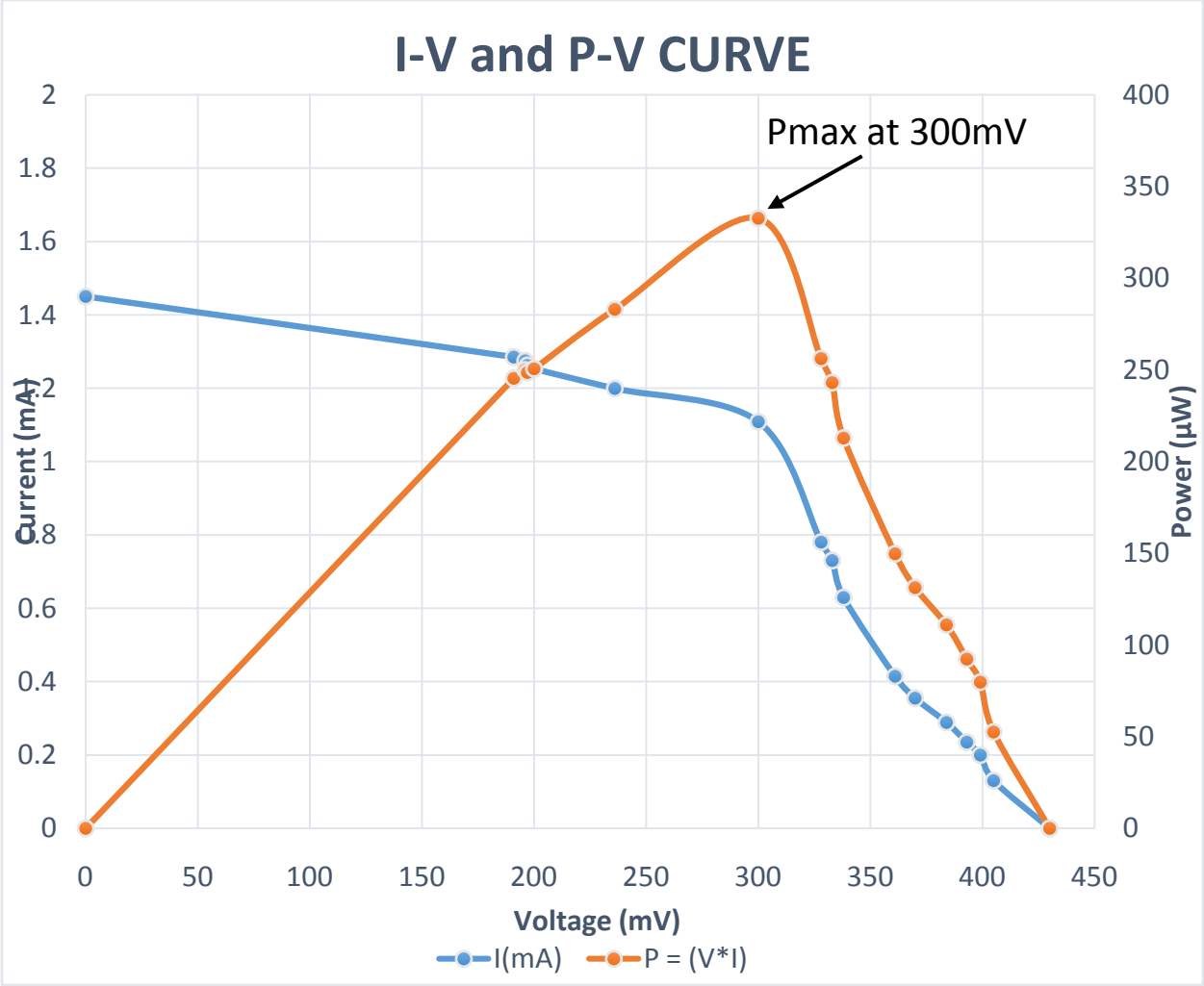

Figure 34: I-V and P-V curves of sample CE4 cell. The sample electrode is prepared from graphite/MWCNT material. This curves represent the electrical properties of this developed cell

Figure 34 represents the I-V characteristics of sample CE4 which has graphite and MWCNT composite material as counter electrode. The I-V curve has shunt loss as well as series loss.

5.4.5 Platinum Sample Analysis

The conventional dye sensitized solar cell uses platinum counter electrode as it shows considerable photoelectric conversion efficiency (PCE). However since it is expensive and rare material, alternative options i.e. carbon material is now under consideration. As a result, to represent comparison data of platinum counter electrode with other carbon electrodes, full cell is developed with platinum counter electrode. The open circuit voltage and short circuit current is measured as described previously. In this fabricated cell Voc=475mV and Isc=0.0972mA from Fig-35.

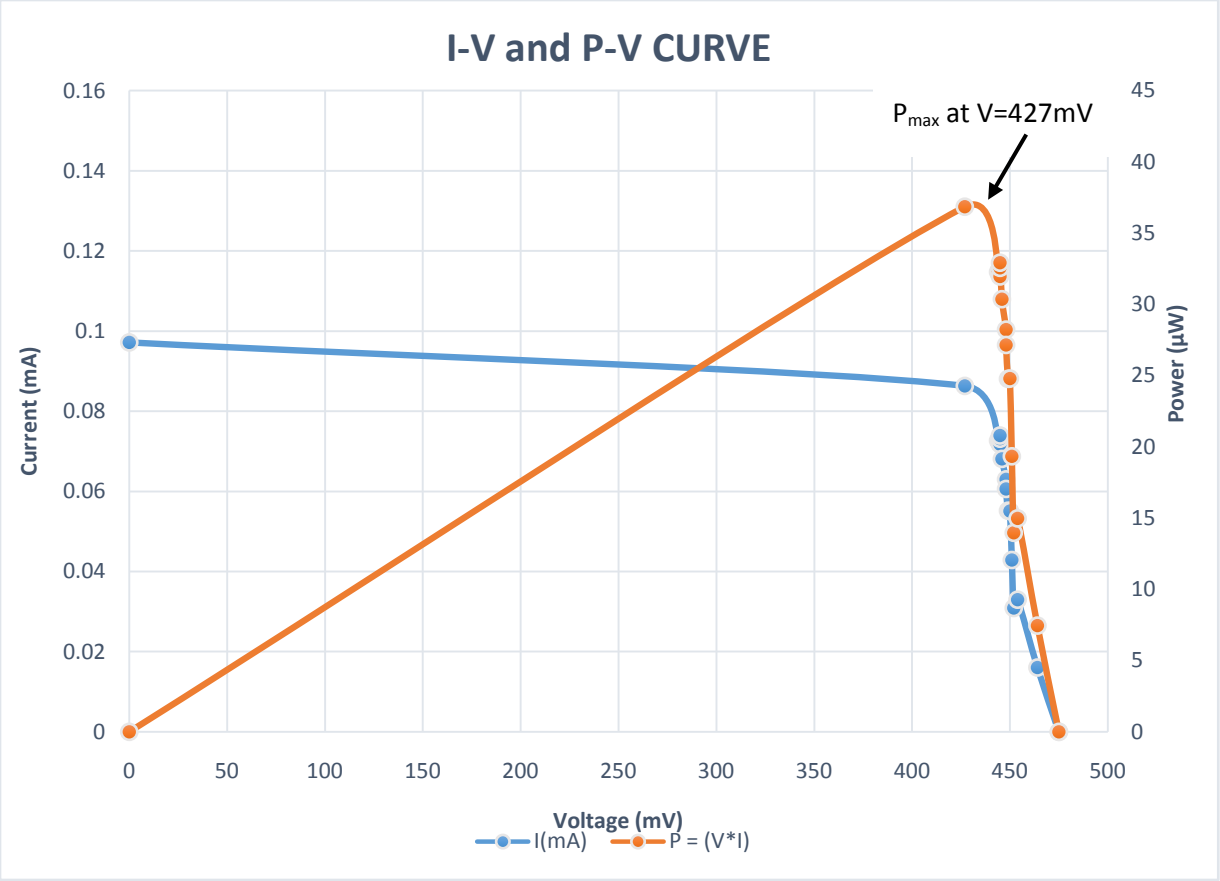

Figure 35: I-V and P-V curves of platinum counter electrode based developed full cell.

Also maximum power point is also identified from the Fig-35. As well as the Vmp and Imp for the maximum power. For this sample Vmp=427mV and Imp=0.0863mA, Pmax=36.8501µW.

5.5 Comparison

Table-2 shortly summarizes the findings from the experimented circuit and calculations.

Table 2: I–V curve characteristics of DSSCs with various counter electrodes

Counter Electrode	Substrate	V_{OC} (mV)	I_{SC} (mA)	Efficiency	Fill Factor	Maximum Power (µW)
CE1	**MWCNT**	450	0.334	0.041	0.83	129.981
CE2	**Graphite**	30	0.146	0.006	0.511	2.2517
CE3	**Graphite: MWCNT**	567	0.1836	0.0139	0.42	43.8
CE4	**Graphite: MWCNT**	430	1.45	0.0832	0.533	332.7
Reference Electrode	**Platinum**	475	0.0972	0.01	0.798	36.850

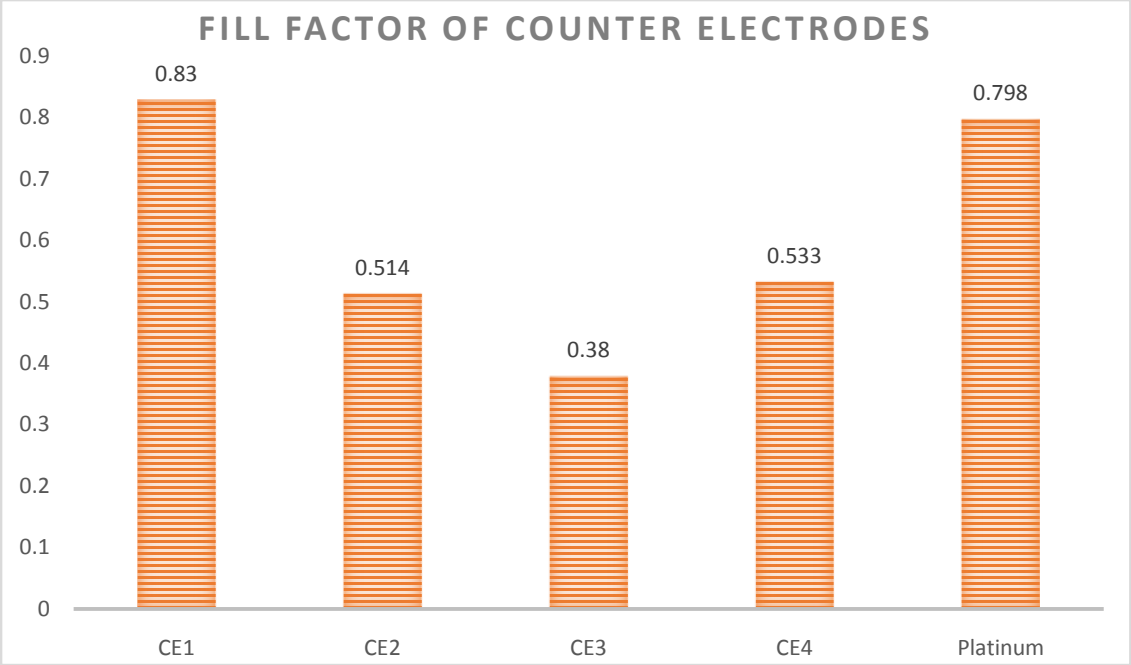

Figure 36: Fill factor comparison among 5 types of counter electrodes based developed cell.

Fig-36 brings all the fill factor information in a bar chart. Here it can be seen that CE1 counter electrode shows highest fill factor which is quite closer of the platinum counter electrode's fill factor. After that sample CE4 shows closer fill factor which is 0.533.

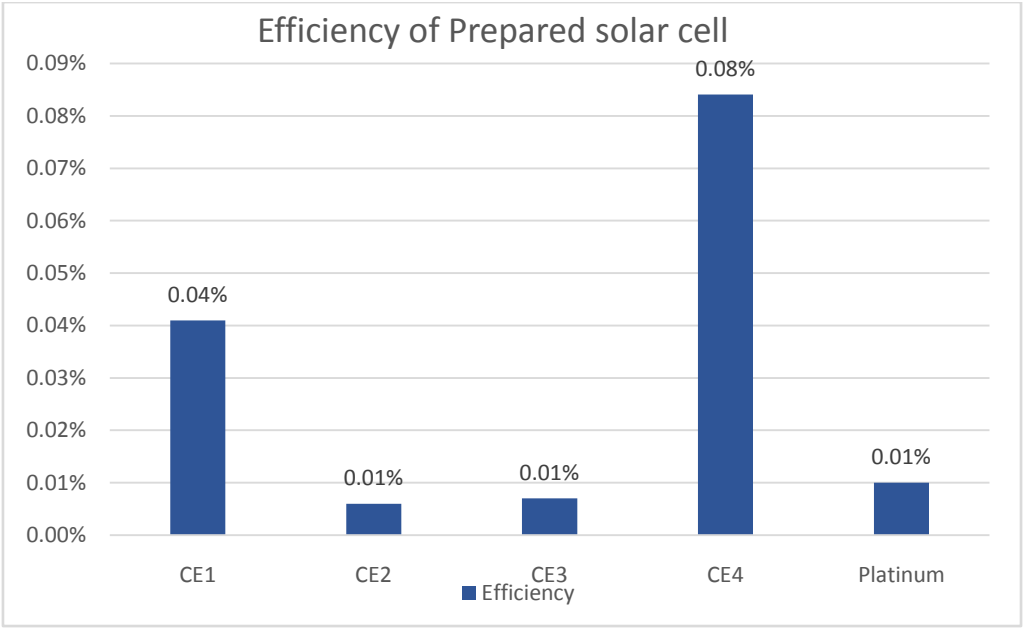

Figure 37: Photoelectric conversion efficiency among 5 different kind of DSSC. Here only counter electrodes are varied and their efficiencies are calculated

Here in Fig-37, all the photo conversion efficiencies of the prepared cells are brought together in a bar chart. From the image it can be seen that sample CE4 shows the highest efficiencies among

them. Also it shows higher efficiency than the platinum counter electrode. After that sample CE1 presents quite noticeable efficiency. Among them sample CE2 is the lowest one to provide conversion efficiency.

5.6 Discussion

The photo conversion efficiencies are tested with the Indian Blackberry dye act as a sensitizer. Among the counter electrodes sample CE1 and CE4 shows relatively good results in consideration with open circuit voltage, short circuit current, FF and efficiency. However sample CE4 shows moderate fill factor and high photo conversion efficiency among them. It also exceeds the platinum electrode's efficiency and have moderate fill factor. Thus sample CE4 is suggested for future use.

5.7 Conclusion

In this chapter graphical analysis and calculations are done to explore the effect of electrical performance of four types of dye sensitized of solar cells. Here only the counter electrodes are varied keeping the TiO_2 anode and Blackberry dye unchanged.

Chapter-6: Conclusion

In this chapter concluding remarks of the thesis work will be given. Section 6.1 will be focused on the finding from the lab work. Where section 6.2 will give a short overview of the problems faced in the laboratory while fabricating. Section 6.3 expresses optimum cost overview of the fabrication and lastly 6.4 will give concluding summary.

6.1 Findings

1. Four different types of counter electrodes have been tested. Their open circuit voltage and short circuit current parameters are

MWCNT based counter electrode: V_{OC}=450mV and I_{SC} =.334mA

Graphite based counter electrode: V_{OC}= 30mV and I_{SC}=0.146mA

Graphite: MWCNT ratio of3:1 based counter electrode: V_{OC}= 567mV and I_{SC}=0.1836mA

Graphite: MWCNT ratio of 3:1 (with PEG) based counter electrode: V_{OC}=430mV and I_{SC}=1.45mA

2. Among the 4 types of counter electrodes 3:1 ratio of graphite and MWCNT (with PEG) based counter electrode is suggested for its better photo conversion efficiency.

3. For the use of sensitizer, locally available, low cost Blackberry dye shows a noticeable effect in photo electric performance. Thus the dye can also be suggested for using in future.

6.2 Problems

While working on the preparation of the counter electrodes some problems occurred that hampered the fabricating process in some length. Also it affected the photo electric performance of the cells.

- The main challenge that has arose while fabricating is the coating thickness control. There is no way of controlling coating thickness precisely which results in low performances at the end.
- In this experimental work doctor blading techniques followed manually using a glass rod. But glass rod cannot provide uniform deposition all over the ITO glass. Also manual it is tough to coat uniformly.
- Here for sample CE2, CE3 and CE4 graphite was used for deposition and thus carbon rods of used batteries are crushed into pieces for about 20 minutes. In sample CE2 where only graphite is used had rough surface. The reason lies on the size of the graphite particles.

- Doctor blade deposition method requires paste or suspension substrate for coating and problems were faced during the preparation of the paste. Later optimization is done by applying polyethylene glycol (PEG) as binder.
- Electrolyte used in this work is liquid. Thus it evaporates quickly. Also no sealant was available at that time to close the edge of the cells.
- While testing the photo conversion efficiency in the solar simulator the probes connected for measurement makes some electrical losses. Due to which the actual data is not being able to pull down from the simulator.

6.3 Future Scope

There has been a great deal of recent success developing organic dye sensitized solar cells with natural dye. Among counter electrode materials Platinum are popular due to its properties required for the DSSC function, it has become more challenging to find its substitute. However some carbon based materials are suggested in this thesis work for the replacement. Thus the key in the future will be in developing more efficient carbon based counter electrode. However some more future scopes of developing the sector is-

- The coatings of the both electrodes are done with glass rods. However screen printing techniques will be an efficient method for increasing efficiency.
- Cell area has noticeable effect on the performance of the DSSC. Thus research on the cell area can also be considered as important.
- Other carbon materials such as graphene can also be included the process and research can be done on the effects of it.
- Ratios of the carbon materials can be varied to observe their photo conversion performance.
- Research can be done on the cell resistance and variation of annealing temperature of the counter electrode.
- Glass substrate of the DSSC can be replaced by flexible substrate which will ease the application of DSSC.

6.4 Conclusion

According to my research it is clear that the best combination of a dye sensitized solar cell fabrication is TiO_2 coated photo anode, Blackberry dye and 3:1 ratio of graphite:MWCNT with PEG coated counter electrode. In this combination we achieve maximum open circuit voltage of 430 mV. However the resistance of this solar cell is relatively high and the efficiency of the solar cell is relatively low. So, the reduction of resistance of the cell and the improvement of efficiency are considered as its next research.

References

[1] S. Zhang, X. yang, Y. Numata and L. han, "Highly efficient dye-sensitized solar cells: progress and future challenges," *Energy Environ. Sci*, vol. 6, no. 5, p. 1443, 2013.

[2] M. Hara, "Biomass conversion by a solid acid catalyst," *Energy & Environmental Science* , vol. 3, no. 5, p. 601, 201.

[3] D. L. P. C. J. E. M. F. W. J. S. H. S. a. M. G. U. Bach, "Solid-state dye-sensitized mesoporous TiO2 solar cells with high photon-to-electron conversion efficiencies," *Nature,* vol. 395, no. 6702, p. 583, 1998.

[4] L. Grandell and M. Höök, "Assessing Rare Metal Availability Challenges for Solar Energy Technologies," *sustainability*, vol. 7, pp. 11818-11837, 2015.

[5] B. G. S. L. K. L. a. P. H. Hagfeldt A., "Dye-Sensitized Solar Cells," *Chemical Reviews,* pp. 6595-6663, 2010.

[6] Z. L. C. Q. Q. Q. Joshi P., "Electrospun Carbon Nanofibers as Low-Cost Counter Electrode for Dye-Sensitized Solar Cells," *ACS Applied Materials & Interfaces,* pp. 3572-7, 2010.

[7] S. A. A. D. Noked M., "The electrochemistry of activated carbonaceous materials: past, present, and future," *Journal of Solid State Electrochemistry,* p. 1563, 2011.

[8] T. N. Murakami, S. Ito, Q. Wang, M. K. Nazeeruddin, T. Bessho, I. Cesar, P. Liska, R. Humphry-Baker, P. Comte, P. Péchy and M. Grätzelz, "Highly efficient dye-sensitized solar cells based on carbon black counter electrodes.," *Journal of Electrochem Soc,* p. A2255–A2261, 2006.

[9] I. S., "Helical microtubules of graphitic carbon," *Nature,* pp. 354:56-8, 1991.

[10] W. X. C. Z. W. M. Y. Y. Li WZ, "Pt–Ru supported on double-walled carbon nanotubes as high performance anode catalysts for direct methanol fuel cells," *Journal of Physical Chemistry B,* pp. 110:15353-8, 2006.

[11] E. R. D. Y. L. J. S. S. W. J. Lee, "Efficient Dye-Sensitized Solar Cells with Catalytic Multiwall Carbon Nanotube Counter Electrodes," *ACS Appl. Mater. Interfaces,* p. 1145, 2009.

[12] K. B. a. S.-W. R. G. Veerappan, "Sub-micrometersized graphite as a conducting and catalytic counter electrode for dye-sensitized solar cells," *ACS Applied Materials and Interfaces,* pp. 857-862, 2011.

[13] K. Imoto, K. Takahashi, T. Yamaguchi, T. Komura, J. Nakamura and K. Murata, "High performance carbon counter electrode for dye-sensitized solar cells," *Sol Energy Mater Sol*

Cells, pp. 459-469, 2003.

[14] Y. X. L. S. C. M. H. A. W. L. a. S. L. Teng C, "Tuning the HOMO Energy Levels of Organic Dyes for Dye-Sensitized Solar Cells Based on Br − /Br 3 − Electrolytes," *Chemistry - A European Journal* , vol. 44, no. 16, p. 13128, 2010.

[15] J. Halme, *Dye-sensitized nanostructured and organic photovoltaic cells:technical review and preliminary tests,* Helsinki, 2002.

[16] E. Arsenault, *Three-Dimensional Transparent Conducting Oxide Based Dye Sensitized Solar Cells,* Toronto, 2011.

[17] Y. H. S. C. C.M. Chen, "Effects of annealing conditions on the properties of TiO2/ITO-based photoanode and the photovoltaic performance of dye-sensitized solar cells," *Journal of Alloys and Compounds,* p. 873, 2011.

[18] S. Yoon, S. Tak, J. Kim, Y. Jun, K. Kang and J. Park, "Application of transparent dye-sensitized solar cells to building integrated photovoltaic systems," *Building and Environment,* p. 1899, 2011.

[19] "Indoor Dye Sensitized Solar Cells," 18 July 2016. [Online]. Available: http://gcell.com/dye-sensitized-solar-cells/advantages-of-dscc/indoor-dye-sensitize-solar-cells.

[20] S. J., "World's first commercial application of DSSC solar technology is in the bag," New Atlas, 2009.

[21] S. K. Ramamurthy V., Semiconductor Photochemistry And Photophysics, CRC Press, 2003.

[22] Z. Chen, W. Li, R. Li, Y. Zhang, G. Xu and H. Cheng, "Fabrication of Highly Transparent and Conductive Indium–Tin Oxide Thin Films with a High Figure of Merit via Solution Processing," *Langmuir,* p. 13836–13842, 2013.

[23] G. S. ,. J. v. d. L. ,. H. M. C. ,. A. M. ,. a. A. J. F. N.-G. Park, "Dye-Sensitized TiO2 Solar Cells: Structural and Photoelectrochemical Characterization of Nanocrystalline Electrodes Formed from the Hydrolysis of TiCl4," *The Journal of Physical Chemistry,* pp. 3308-14, 1999.

[24] Y. Wang, J. Wu, Z. Lan, Y. Xiao, Q. Li, F. Peng, J. Lin and M. Huang, "Preparation of porous nanoparticle TiO2 films for flexible dye-sensitized solar cells," *Chinese Science Bulletin,* vol. 56, no. 24, pp. 2649-2653, 2011.

[25] N. A. K. G. P. S. a. L. B. Ishwar Chandra Maurya, " Natural Dye Extracted From Saraca asoca Flowers as Sensitizer for TiO2-Based Dye-Sensitized Solar Cell," *Journal of Solar Energy Engineering,* p. 138, 2016.

[26] D. P. R. M. J. O. V. d. F. I. A. Ana Faria, "Influence of anthocyanins and derivative pigments from blueberry (Vaccinium myrtillus) extracts on MPP+ intestinal uptake: A structure–activity approach," *Food Chemistry*, pp. 587-594, 2008.

[27] A. A.-A. M. A. B. M. A. A. H. K. K. S. N. S. A. K. Norasikin A. Ludin, "Review on the development of natural dye photosensitizer for dye-sensitized solar cells," *Renewable and Sustainable Energy Reviews*, pp. 386-396, 2014.

[28] M. A. Khan and M. S. Akhtar, "Synthesis, characterization and applicable of sol-gel derived mesoporous TiO2 nanoparticles for dye-sensitized solar cells," *Solar Energy*, vol. 84, pp. 2195-2201, 2010.

[29] M. Matsumoto, Y. Wada, T. T. Kitamura, K. Shigaki, T. Inoue, M. Ikeda and S. Yanagida, "Fabrication of solid-state dye-sensitized TiO2 solar cell using polymer electrolyte," *Bulletin of the Chemical Society of Japan* , vol. 74, pp. 387-393, 2001.

[30] M. R. Al-bahrani, W. Ahmad, H. Fatima Mehnane, Y. Chen, Z. Cheng and Y. Gao, " Enhanced Electrocatalytic Activity by RGO/MWCNTs/NiO Counter Electrode for Dye-sensitized Solar Cells," *Nano-Micro Letters*, vol. 7, no. 3, pp. 298-306, 2015.

[31] S. S., "Scanning Electron Microscopy (SEM)," [Online]. Available: http://serc.carleton.edu/research_education/geochemsheets/techniques/SEM.html.

[32] F. Liu, J. Wu, K. Chen and D. Xue, "Morphology Study by Using Scanning Electron Microscopy," *Microscopy: Science, Technology, Applications and Education*, pp. 1781-1792, 2010.

[33] W. J. Qi B., "Open circuit voltage in organic solar cells," *Journal of Materials Chemistry*, 2012.

APPENDIX

I-V and P-V curve data:

CE1			CE2			CE3		
V(mV)	I(mA)	P(μW)	V(mV)	I(mA)	P(μW)	V(mV)	I(mA)	P(μW)
0	*0.334*	*0*	0	*0.146*	*0*	0	*0.1836*	*0*
394	0.3299	129.981	20	0.106	2.12	438	0.1	43.8
395	0.329	129.955	22.5	0.099	2.2275	468	0.081	37.908
402	0.277	111.354	23.8	0.094	2.2372	487	0.061	29.707
406	0.2309	93.7454	24.1	0.093	2.2413	489	0.0576	28.1664
410	0.198	81.18	25.3	0.089	2.2517	490	0.0571	27.979
414	0.176	72.864	27.5	0.08	2.2	493	0.0568	28.0024
418	0.156	65.208	27.7	0.076	2.1052	494	0.0562	27.7628
421	0.1396	58.7716	27.9	0.061	1.7019	496	0.056	27.776
425	0.124	52.7	28	0.054	1.512	498	0.0558	27.7884
430	0.117	50.31	28.2	0.05	1.41	500	0.0557	27.85
431	0.1054	45.4274	28.5	0.044	1.254	502	0.0549	27.5598
437	0.101	44.137	28.9	0.0036	0.10404	503	0.0532	26.7596
437	0.0948	41.4276	29	0.003	0.087	504	0.052	26.208
439	0.089	39.071	29.2	0.0024	0.07008	505	0.0518	26.159
440	0.0878	38.632	29.5	0.0017	0.05015	510	0.048	24.48
450	*0*	*0*	30	*0*	*0*	567	*0*	*0*

CE4			Platinum		
V(mV)	I(mA)	P(μW)	V(mV)	I(mA)	P(μW)
0	*1.45*	*0*	*0*	*0.0972*	*0*
191	1.285	245.435	427	0.0863	36.8501
196	1.275	249.9	444	0.0727	32.2788
197	1.262	248.614	445	0.072	32.04
200	1.253	250.6	445	0.0718	31.951
236	1.199	282.964	445	0.0732	32.574
300	1.109	332.7	445	0.074	32.93
328	0.781	256.168	446	0.0681	30.3726
333	0.73	243.09	448	0.063	28.224
338	0.63	212.94	448	0.0606	27.1488
361	0.415	149.815	449	0.0552	24.7848
370	0.355	131.35	450	0.0551	24.795
384	0.289	110.976	451	0.0429	19.3479
393	0.235	92.355	452	0.0309	13.9668
399	0.2	79.8	454	0.033	14.982
405	0.13	52.65	464	0.0161	7.4704
430	*0*	*0*	*475*	*0*	*0*